Supporting Methods

RNA-seq of *N. vitripennis* and *N. giraulti* adult whole body samples.

Total RNA samples were extracted from a pool of 10 adult whole-body samples 24 h following eclosion from *N. vitripennis* (strain AsymCX) and *N. giraulti* (strain R16A) males and females, using Qiagen RNeasy Plus mini kit (Qiagen, CA). Three independent biological replicates were performed for each species and each sex (*SI Appendix*, Table S1). RNA concentrations and A260/A280 absorption ratios were measured with a NanoDrop ND-1000 Spectrophotometer (Thermo Scientific, DE). RNA integrity was tested using an Agilent 2100 Bioanalyzer (Agilent Technologies, CA). RNA-Seq libraries were made from 2 ug total RNA input using TruSeq RNA Sample Preparation Kits v2 (Illumina Inc., CA), and sequenced on an Illumina HiSeq2000 instrument following standard Illumina RNA-seq protocols.

WGBS-seq of *N. vitripennis* and *N. giraulti* adult whole-body samples.

Genomic DNAs were extracted from a pool of 50 adult whole-body samples 24 h after eclosion of *N. vitripennis* (strain AsymCX) and *N. giraulti* (strain R16A) males and females, using the DNeasy Blood & Tissue Kit (Qiagen, CA). The DNA A260/A280 absorption ratios were measured with a NanoDrop ND-1000 Spectrophotometer (Thermo Scientific, DE) and their concentrations were measured with a Qubit Fluorometer (Life Technologies, CA). For *N. vitripennis* male and female samples, WGBS-seq libraries were made following a custom protocol described in our previous work (1) (*N. vitripennis* female data is under GEO accession no. GSE43423), with 20 ug input DNA and Illumina PE adapters. Each library was sequenced in one GAIIx and one HiSeq2000 lanes (*SI Appendix*, Table S4). 0.5% of non-methylated control lambda DNA (Cat No.

D1521, Promega, WI) was mixed in the libraries and the bisulfite conversion efficiency is 99.7% (1). For *N. girault*i male and female samples, WGBS-seq libraries were made according to the Illumina protocols (WGBS for Methylation Analysis Guide, Part# 15021861 Rev. A) with 15 ug of starting DNA and Illumina TruSeq adapters. We added a size selection step (130-180 bp) after DNA fragmentation to the Illumina protocol. WGBS-seq libraries were pooled and sequenced in 3/4 HiSeq2000 lane (*SI Appendix*, Table S4). The bisulfite conversion rate, estimated from non-methylated lambda controls, was found to be 99.90%.

RNA-seq read alignments and data analysis.

Illumina sequence QC was performed using FastQC software (2). 1-3% adapter containing reads were trimmed by Trimmomatic (3) (*SI Appendix*, Table S1). The reads were then aligned to *N. vitripennis* and *N. girault*i reference genomes (v1.0) (4) respectively using TopHat v2.0 (5) and ~90% of them were uniquely mapped to the genome (*SI Appendix*, Table S1). Counts of aligned reads in *Nasonia* OGS2 (official gene set 2) transcripts (1, 6) were summarized by Cufflinks v2.1.0 (7) and reads mapped to multiple places in the genome were weighted by the "-u" parameter. Since multiple mapped reads may have significant effect on the paralogs of extremely highly expressed genes, we summarized the counts from uniquely mapped reads only. We also summarized the gene counts based on OGS2 gene models by two additional software packages, HTSeq (8) and BEDTools (9), and the result is robust to different read counts summary methods. Read counts for fewer than 30 genes disagreed among these three programs, and we manually corrected them. These read counts were fed into the edgeR package in Bioconductor (10, 11). Normalization was performed and total expression

levels (FPKM: Fragments Per Kilobase-pair of exon Model) were calculated using edgeR. After filtering out the non-expressed or extremely lowly expressed genes in all samples (FPKM<1 in all replicates), a total of 16,400 genes were covered in the RNA-seq data in the two species. Differentially expressed genes between the two sexes and the two species were detected by edgeR using 5% FDR (false discovery rate, *q*-value<0.05). Using all mapped reads and uniquely mapped reads gave almost identical results, which is consistent with the high mapping percentage (~90%) for uniquely mapped reads (*SI Appendix*, Table S1). Testis RNA-seq data from *N. vitripennis* were downloaded from Sequence Read Archive (SRA) with accession number SRX325702 (12) and analyzed using the same pipeline.

Arbitrary cut-offs were selected for the SB+ and SS gene categories based on previous literature and trials of different cut-offs. For SB+ genes, we tried 8-fold, 10-fold, 12-fold and 15-fold cut-offs and the same trend was observed for all values. 8-fold was used in the final analysis because it is already a high fold change and only a few genes pass this threshold in other published studies, such as in *Drosophila*. For SS genes, the actual number of fold difference is meaningless, because of the extremely low expression level in one sex. According to the definition of sex-specific expression, we used the criteria of "present in one sex and absent in the other" to set the cut-off. We tried several combinations of cut-offs, including FPKM < 0.1, 0.2, 0.4, 0.5, 1.0 for lowly expressed genes, and FPKM > 1, 2, 3, 4 for highly expressed ones. The same trend/results were observed for different cut-offs, suggesting that the conclusions of the paper are robust to these cut-off choices. To determine the best cut-off values, we used the following approach: we first checked the actual read coverage for a number of selected genes in

IGV browser for different cut-offs. Then, we compared different FPKM cut-offs in RNA-seq data with expression values from whole-genome expression tiling array data in the same samples. The range of the tiling array expression value is 8.6~15, and to conclude a gene is not present in the microarray data, the widely used criteria in the literature is expression value <9, which matched well with our RNA-seq cut-off.

Validation of differentially expressed genes by qRT-PCR

To confirm sex-biased genes, we designed qRT-PCR primers for nine differentially expressed genes, and these targets were selected to cover both sex-specific and sex-biased candidates (*SI Appendix*, Table S2). The amplicons were designed across exons and qPCR primers were all located in regions without SNPs between *N. vitripennis* and *N. giraulti* to eliminate amplification bias. cDNAs were synthesized from the same total RNA samples used for RNA-seq by SuperScript III Reverse Transcriptase (Life Technologies, CA). qPCR experiments were performed with SYBR Green (Invitrogen, Cat No. S7563) in 384-well plates on a LightCycler 480 Real-Time PCR System (Roche Diagnostics, Germany). Initial analysis was done using the LightCycler 480 Relative Quantification Software. Relative quantification was based on a standard curve for each sample, generated using qPCR results from a dilution series (5 data points) of an unbiased gene (Nasvi2EG003640). The correlation coefficient for the standard curve was high in all samples (R^2>0.98). Each sample had three biological and two technical replicates.

WGBS-seq read alignments and analysis of DNA methylation.

-WGBS-seq alignments. Illumina read QC was performed using FastQC software (2). For *N. vitripennis* male and female data, ~14% adapter containing reads were trimmed by

Trimmomatic (3) (*SI Appendix*, Table S4). We then aligned the reads to the converted *N. vitripennis* reference genome (v1.0) using BWA (13) allowing up to 4 mismatches per read. A detailed protocol can be found in our previous publication (1). For *N. giraulti* male and female data, fewer than 4% of adapters were trimmed and the remaining reads were aligned to the converted genomes replaced by *N. giraulti* alleles at SNP positions. To accommodate indels between *N. vitripennis* and *N. giraulti*, a different set of parameters were used in BWA alignments allowing a total of 6 mismatches (*SI Appendix*, Table S4). ~85% of all the reads were aligned to the converted genomes in both species and only ~65% of those that uniquely mapped to the genome were kept for the methylation analysis. For uniquely mapped reads with indels, we queried the indel position against the indel database and unmatched spurious indels due to misalignment were excluded. In the end, 50-60% of the reads survived these QC filtering steps and they were summarized in a single BAM file for methylation analysis (*SI Appendix*, Table S4). The aligned BAM files were viewed in the IGV browser (14, 15).

-Quantification of genome DNA methylation at CpG level. Of the 14,024,488 CpG sites in *Nasonia* haploid genome, we only included CpG sites covered by the Illumina genome DNA sequencing data (on samples without bisulfite treatment) in our analysis. CpG sites located in a potential repetitive region were also excluded using a method described in (16), and we ended up with 13,451,035 "alignable" CpGs in *N. vitripennis* and 9,742,004 "alignable" CpGs in *N. giraulti*. 95% of these CpGs were covered by at least one read in all samples, suggesting excellent library complexity (*SI Appendix*, Table S5 and Fig. S5). We define **coverage CpGs** as CpGs with a read depth of 10 or more for *N. vitripennis* samples and a read depth of 15 or more for *N. giraulti* samples. To measure the degree of

DNA methylation at the individual CpG level, **methylation percentage** was calculated at each CpG by unconverted Cs over the total coverage. To achieve accurate estimation of methylation percentage, only covered CpGs were included in the analysis, and they account for more than 50% of the total CpGs (*SI Appendix*, Table S5). To assign a binary status of methylation at CpG sites, we define **methylated CpGs (mCpGs)** as covered CpG sites with >30% methylation. This arbitrary cut-off is based on the distribution of methylation percentage we observed in our data (*SI Appendix*, Fig. S6). According to this criterion, 1~2% of the seven million covered CpG sites were methylated in *Nasonia* genome.

-Analysis of gene methylation status. From our previous work, DNA methylation in *Nasonia* is enriched in coding exons at the beginning of genes (1). Based on this pattern, we define genes with >10% methylated CpGs in the first 1 kb coding region as **methylated genes**, and genes with ≤ 10% methylated CpGs in the first 1 kb as **non-methylated genes.** CpG sites present in overlapping gene models (8% of all CpGs) were excluded from the analysis. According to these criteria, methylation status was determined for ~16,000 OGS2 genes in *N. vitripennis* and ~14,000 genes in *N. giraulti*. Methylation status was not assigned to genes with fewer than 4 covered CpGs in the first 1 kb coding region.

Validation of sex- and species-differentially methylated candidate genes using cloning and Sanger sequencing method and PyroMark assay.

For bisulfite sequencing using cloning and Sanger sequencing methods, PCR primers were designed using the Methyl Primer Express Software v1.0 (Life Technologies, CA). Detailed bisulfite sequencing protocols can be found in (1). For DNA methylation

quantification using the PyroMark assay, genomic DNA samples were extracted from a pool of 50 24 h post-eclosion adult males and females for both *N. vitripennis* and *N. giraulti* using the Qiagen DNeasy Blood and Tissue Kit (Cat No. 69504). Two biological replicates were done for each sample and they are independent of the WGBS-seq samples. Bisulfite conversion was carried out on 2 ug input genomic DNA in both sexes of both species with the Qiagen EpiTect Bisulfite Kit (Qiagen, CA). PyroMark primers were designed to target candidate differentially methylated CpGs (Supplemental Table S6) with PyroMark Assay Design Software Version 2.0.1.15 (Qiagen, CA). PCR products were prepared, run and analyzed on the PSQ 96MA Pyrosequencer (Qiagen, CA) with PyroMark CpG software 1.0.11. Background subtraction was done using the "control peak heights" feature. Two technical replicates were performed for each sample.

Phylogenetic analysis of the fatty acid desaturase gene family in *Nasonia* and other insects.

15 fatty acid desaturase gene family members in *Nasonia* were identified by >35% protein sequence identity with Nasvi2EG017727. Protein sequences of 7 orthologous genes in honeybee (*Apis mellifera*), 9 in ant (*Camponotus floridanus*) and 6 in fly (*Drosophila melanogaster*) were obtained from OrthoDB7 (17). These sequences were aligned using ClustalW (18) and an unrooted Neighbor-Joining tree (Fig. 2B) was constructed n MEGA5 (19).

Recombination intensity and evolutionary analysis of sex-biased genes in *Nasonia*.

Nasonia paralog and *Nasonia-Apis* ortholog status was from the *Nasonia* OGS2 dataset (http://arthropods.eugenes.org/EvidentialGene/nasonia/) (6). Synonymous (dS) and non-synonymous substitution rates (dN) between *N. vitripennis* and *N. giraulti* were estimated

using `codeml` in PAML 4.7 (20) for 12,469 perfectly aligned OGS2 genes with no indels. To estimate local recombination intensity, *Nasonia* chromosomes were assembled from v2 scaffolds in NCBI, based on the current linkage map with more than 20,000 markers (21). Unlike NCBI assembly v2.1 (GenBank Acc. ID: GCA_000002325.2), mapped but unordered scaffolds were kept in the assembly, most of which are short or centromeric scaffolds. For each chromosome, genetic map distances (cM) were plotted against physical distance (Mbp) (Fig. 6A) and local regression was performed to fit the curve using the `Locfit` package in the R with the following parameters: bandwidth = 0.06, local polynomial degree = 2; weight function: tricube. Local recombination intensities were calculated as the first derivative of the fitted line for each chromosome.

Supporting Text. Lack of strong and stable sex-differences in DNA methylation

We noticed that the methylation differences for sex-DM candidate genes (Fig. 3B) were much lower compared to the species-specific DM candidate genes (Fig. 3C), suggesting that the sex-DM candidates might be due to sampling variability, tissue-specific differences in methylation, or local bisulfite conversion artifacts(22). To check this, we examined the sex- and species-differences at individual CpG level and identified sex-differentially methylated CpG sites (sex-DMCpGs) and species-differentially methylated CpG sites (species-DMCpGs) using binomial tests at sites with coverage>15 (see Methods). If the sex-DMCpGs were conserved between species just as the sex-biased expression, a large proportion would be found in both species. In our data, ~15,000 CpG species-DMCpGs are discovered between *N. vitripennis* and *N. giraulti* and more than half are significant in both female and male comparisons (*SI Appendix*, Fig. S7A). In contrast, there are many fewer sex-DMCpGs, and only 8 sites overlapped between the *N. vitripennis* and *N. giraulti* comparisons (*SI Appendix*, Fig. S7A). The results are consistent with the hypothesis that sex-DMCpG candidates are due to random variability or local bisulfite conversion artifacts.

Interestingly, in gene regions, species-DMCpGs are often clustered (*SI Appendix*, Fig. S7B) and they cover almost the entire gene body (*SI Appendix*, Figs. S13-S18), whereas sex-DMCpG candidates rarely cluster in *N. vitripennis* and they do not cluster at all in *N. giraulti* (*SI Appendix*, Fig. S7B). In *N. vitripennis*, clustered sex-DMCpGs tend to locate at the 3'-boundary of the mCpG cluster in methylated genes (*SI Appendix*, Figs. S8-S11). Four such genes with clustered sex-DMCpGs in *N. vitripennis* were selected for validation in independent biological replicates, and we were only able to confirm one

with a much lower magnitude of methylation difference (*SI Appendix*, Table S7 and Figs. 8-S11). These results suggest a lack of strong and detectable differentially methylated genes between the sexes. Sex differences in DNA methylation may be present at specific loci but they were variable across samples.

Supporting References

1. Wang X, *et al.* (2013) Function and evolution of DNA methylation in Nasonia vitripennis. *PLoS genetics* 9(10):e1003872.
2. Andrews S (FastQC A Quality Control tool for High Throughput Sequence Data.
3. Bolger AM, Lohse M, & Usadel B (2014) Trimmomatic: a flexible trimmer for Illumina sequence data. *Bioinformatics* 30(15):2114-2120.
4. Werren JH, *et al.* (2010) Functional and evolutionary insights from the genomes of three parasitoid Nasonia species. *Science* 327(5963):343-348.
5. Kim D, *et al.* (2013) TopHat2: accurate alignment of transcriptomes in the presence of insertions, deletions and gene fusions. *Genome biology* 14(4):R36.
6. Munoz-Torres MC, *et al.* (2011) Hymenoptera Genome Database: integrated community resources for insect species of the order Hymenoptera. *Nucleic acids research* 39(Database issue):D658-662.
7. Trapnell C, *et al.* (2012) Differential gene and transcript expression analysis of RNA-seq experiments with TopHat and Cufflinks. *Nature protocols* 7(3):562-578.
8. Anders SPPTHW (2014) HTSeq - A Python framework to work with high-throughput sequencing data. *bioRxiv*.
9. Quinlan AR & Hall IM (2010) BEDTools: a flexible suite of utilities for comparing genomic features. *Bioinformatics* 26(6):841-842.
10. Nikolayeva O & Robinson MD (2014) edgeR for differential RNA-seq and ChIP-seq analysis: an application to stem cell biology. *Methods in molecular biology* 1150:45-79.
11. Robinson MD, McCarthy DJ, & Smyth GK (2010) edgeR: a Bioconductor package for differential expression analysis of digital gene expression data. *Bioinformatics* 26(1):139-140.
12. Akbari OS, Antoshechkin I, Hay BA, & Ferree PM (2013) Transcriptome profiling of Nasonia vitripennis testis reveals novel transcripts expressed from the selfish B chromosome, paternal sex ratio. *G3* 3(9):1597-1605.
13. Li H & Durbin R (2009) Fast and accurate short read alignment with Burrows-Wheeler transform. *Bioinformatics* 25(14):1754-1760.
14. Thorvaldsdottir H, Robinson JT, & Mesirov JP (2013) Integrative Genomics Viewer (IGV): high-performance genomics data visualization and exploration. *Briefings in bioinformatics* 14(2):178-192.

15. Robinson JT, *et al.* (2011) Integrative genomics viewer. *Nature biotechnology* 29(1):24-26.
16. Wang X & Clark AG (2014) Using next-generation RNA sequencing to identify imprinted genes. *Heredity* 113(2):156-166.
17. Waterhouse RM, Tegenfeldt F, Li J, Zdobnov EM, & Kriventseva EV (2013) OrthoDB: a hierarchical catalog of animal, fungal and bacterial orthologs. *Nucleic acids research* 41(Database issue):D358-365.
18. Larkin MA, *et al.* (2007) Clustal W and Clustal X version 2.0. *Bioinformatics* 23(21):2947-2948.
19. Tamura K, *et al.* (2011) MEGA5: molecular evolutionary genetics analysis using maximum likelihood, evolutionary distance, and maximum parsimony methods. *Molecular biology and evolution* 28(10):2731-2739.
20. Yang Z (2007) PAML 4: phylogenetic analysis by maximum likelihood. *Molecular biology and evolution* 24(8):1586-1591.
21. Desjardins CA, *et al.* (2013) Fine-scale mapping of the Nasonia genome to chromosomes using a high-density genotyping microarray. *G3* 3(2):205-215.
22. Raddatz G, *et al.* (2013) Dnmt2-dependent methylomes lack defined DNA methylation patterns. *Proceedings of the National Academy of Sciences of the United States of America* 110(21):8627-8631.

Supporting Figure S1. M-A plot for expression comparisons between male and female in *N. vitripennis* and *N. giraulti*.

100-fold sex difference lines were drawn for male-biased (blue dots) and female-biased genes (red dots), respectively.

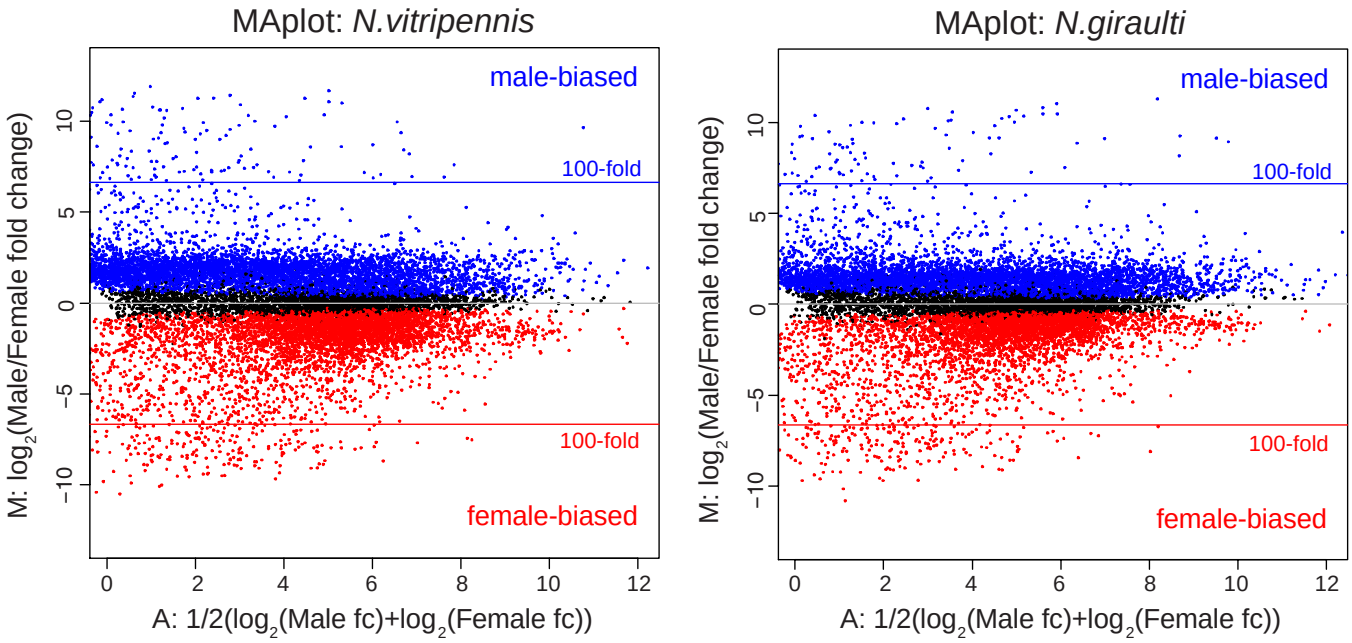

Supporting Figure S2. qRT-PCR validation results for nine selected sex-biased genes in *N. vitripennis* and *N. girault*i.

Male-biased in both species: (A); male-biased only in *N. girault*i: (B); male-specific in both species: (C-E); male-biased only in *N. vitripennis*: (F); male-specific in both species, but the expression is significantly higher in *N. girault*i: (G); female-specific in both species, but the expression is significantly higher in *N. vitripennis* (H); female-specific in both species: (I).

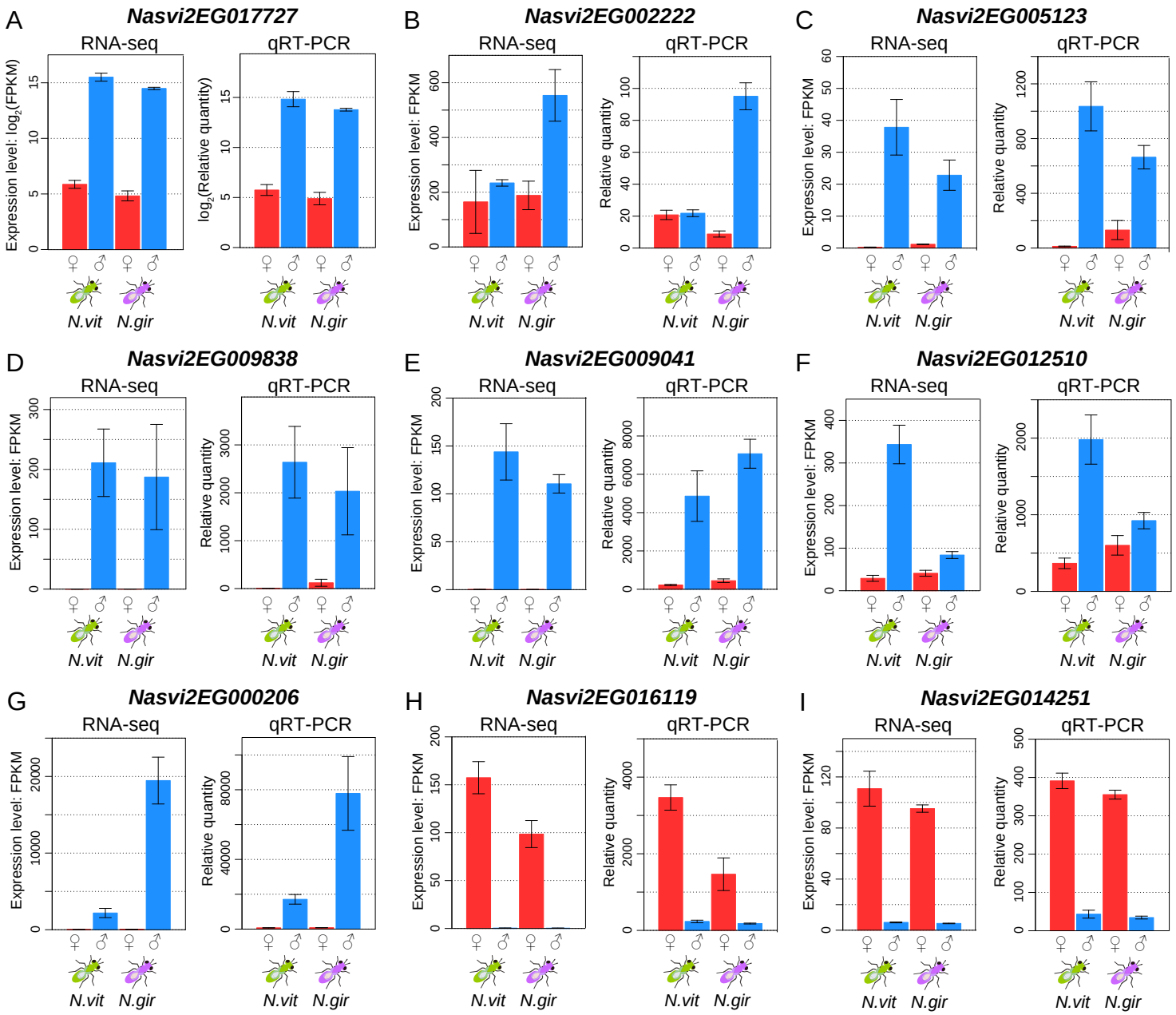

Supporting Figure S3. Gene expression correlation between *N. vitripennis* and *N. girault*i female and male adult samples.

Pairwise scatterplots of the RNA-seq expression level for expressed genes among *N. vitripennis* and *N. girault*i adult females and males (***bottom-left***), color-coded by the point density. Spearman's correlation coefficients are shown in the top-right panels, with text size in proportion to the value.

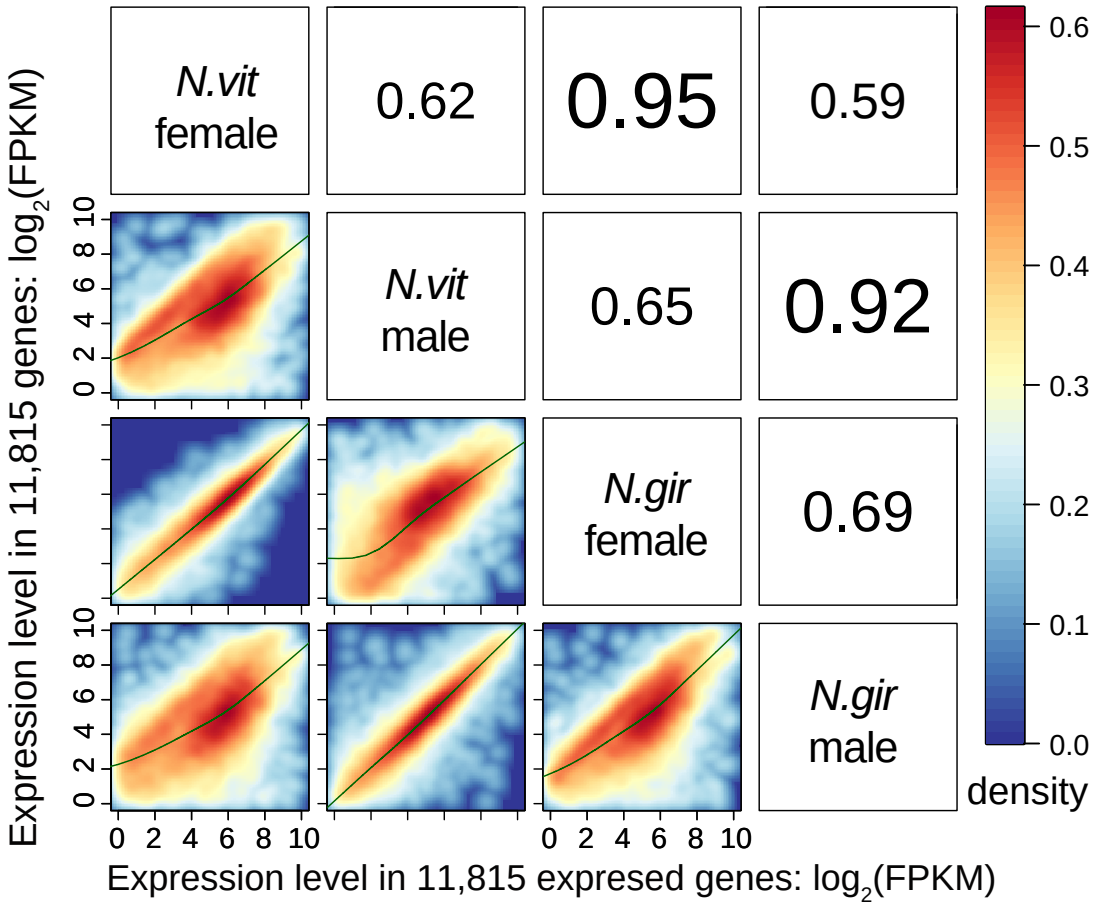

Supporting Figure S4. Sex-biased genes and significantly over-represented GO functional categories for female-specific genes in *N. vitripennis* and *N. giraulti* (adjusted P-value < 0.05).

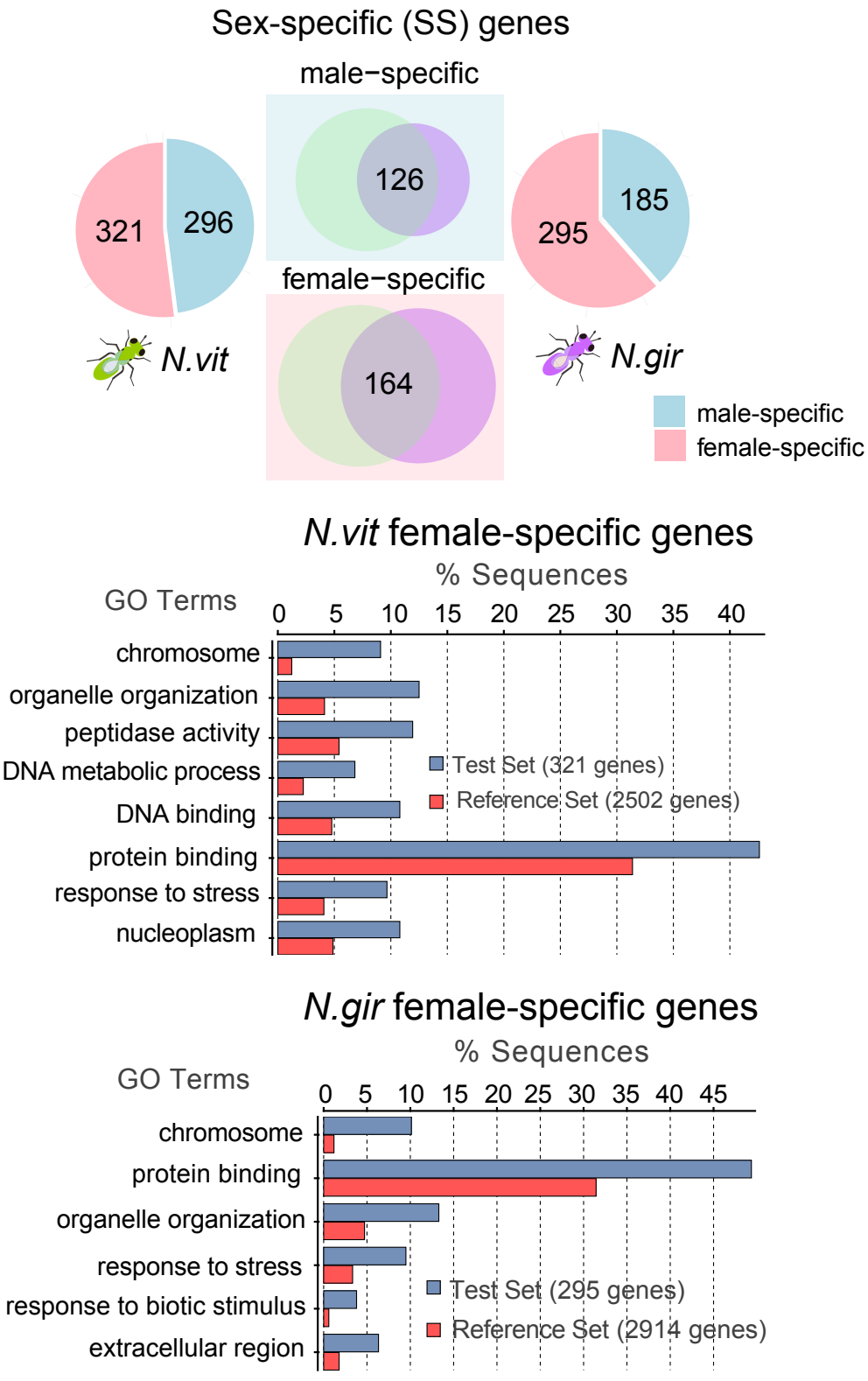

Supporting Figure S5. Distribution of CpG sites coverage in *N. vitripennis* and *N. giraulti* male and female WGBS-seq data.

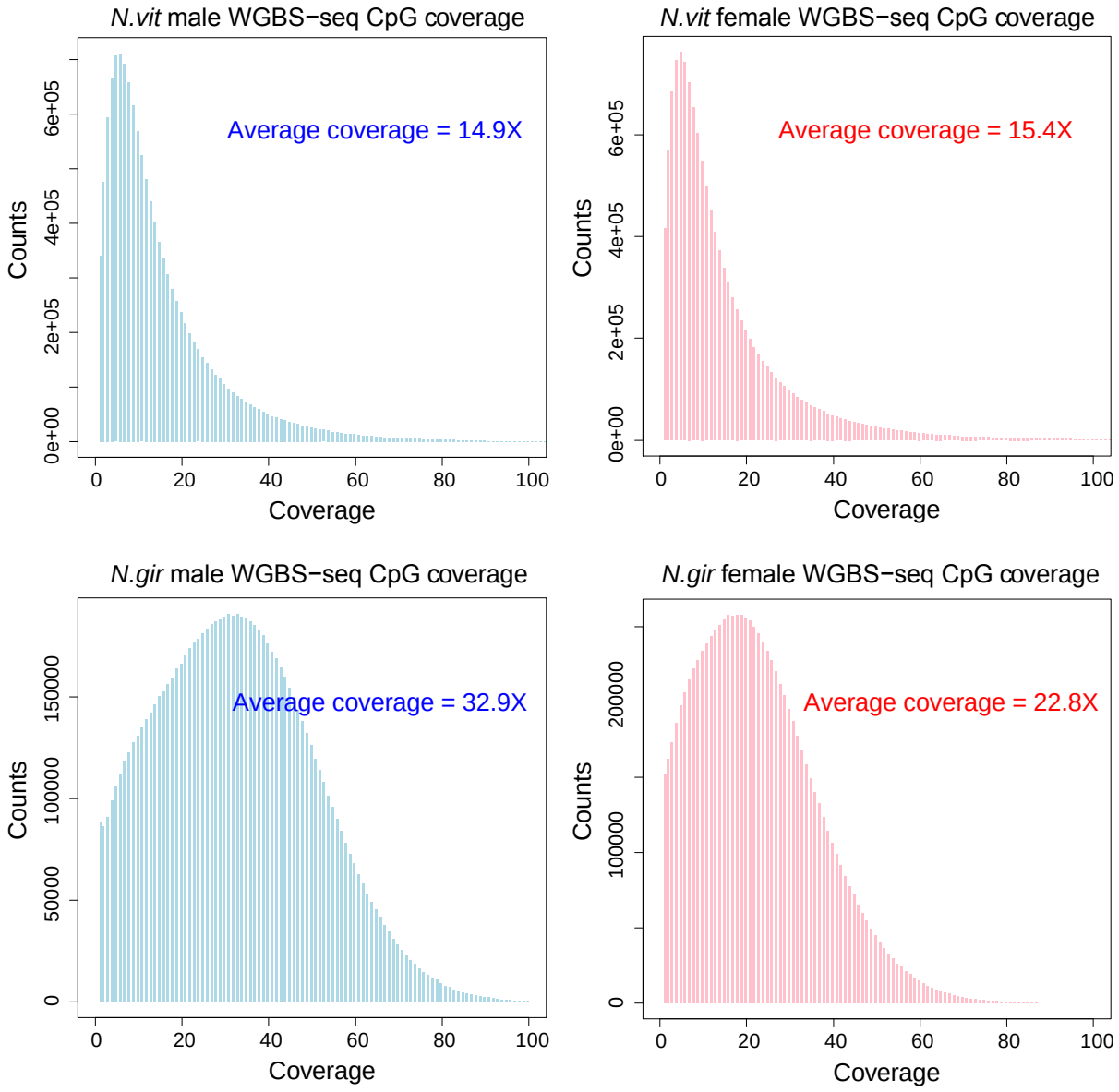

Supporting Figure S6. Distribution of CpG methylation percentages in *N. vitripennis* and *N. giraulti* male and female samples.

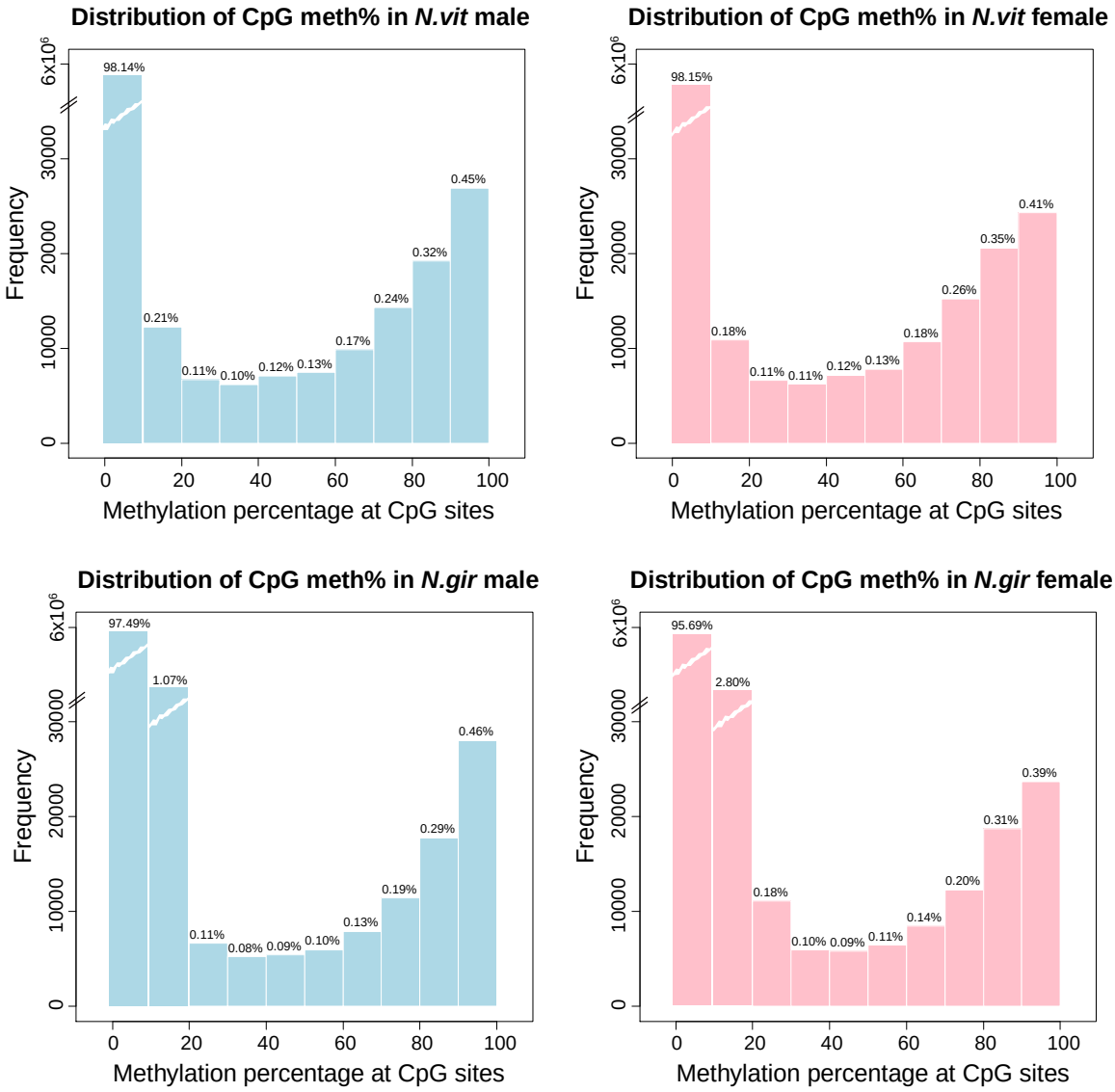

Supporting Figure S7. Distribution and clustering of sex-DMCpGs and species-DMCpGs.

(A) ***Left:*** Venn diagram for significant sex-DMCpGs in *N. vitripennis* and *N. giraulti*.

Right: Venn diagram for significant species-DMCpGs in females and males.

(B) Histograms of sex-DMCpGs in *N. vitripennis* and *N. giraulti* and species-DMCpGs in females and males (from left to right).

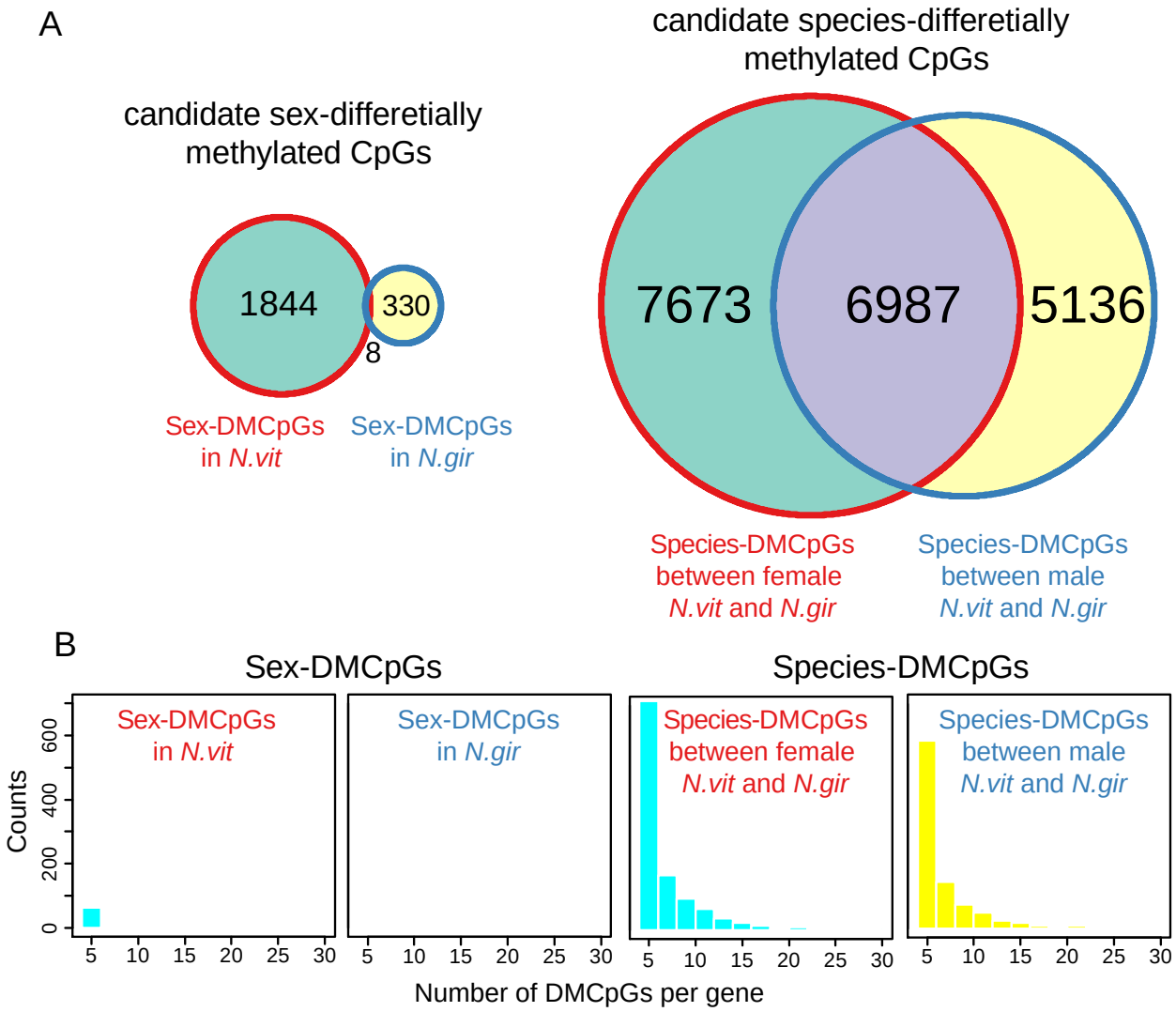

Supporting Figure S8. Validation of CpG methylation status for candidate male-biased methylated gene Nasvi2EG009251 in *N. vitripennis*.

(A) IGV browser screenshot of *N. vitripennis* female (top) and male (bottom) WGBS-seq alignments in a 199 bp region in exon 4 of gene Nasvi2EG009251 on SCAFFOLD17, with 5 CpG sites pointed with blue arrows at the bottom. Two CpGs sites on the left were completely methylated in both sexes, and three CpGs on the right are non-methylated in females but partially methylated in males.

(B) Plots of the gene model, translation start site and CpG methylation profile in both sexes for Nasvi2EG009251 from the WGBS-seq data. A vertical bar was drawn for each CpG at its position in the gene, color-coded by the methylation percentage in proportion to the bar length (blue: methylated Cs; red: non-methylated Cs that were converted to Ts). From this plot, Nasvi2EG009251 is methylated in both females and males, with the majority of the methylation within 5'-1kb coding region. 346 CpGs covered with 6 or more depth were shown here, and 12 significantly differentially methylated between sexes (DMCpGs, within the orange box) are located at the 3'-boundary of the methylated CpG cluster.

(C) Bisulfite sequencing verification results for the 5 CpGs sites shown in (A) using the cloning and Sanger sequencing method in both sexes from an independent biological replicate. The estimated methylation percentages at each CpG site from the WGBS-seq and single-gene bisulfite sequencing were shown on the top. At the three DMCpG sites, male methylation profile matched well, but in females they display much higher percentage of methylation (37% on average) than in the WGBS-seq data (3% on average). Therefore, the sex differences in DNA methylation was validated, but at a much lower degree (27% on average) compared to the WGBS-seq data (62% on average).

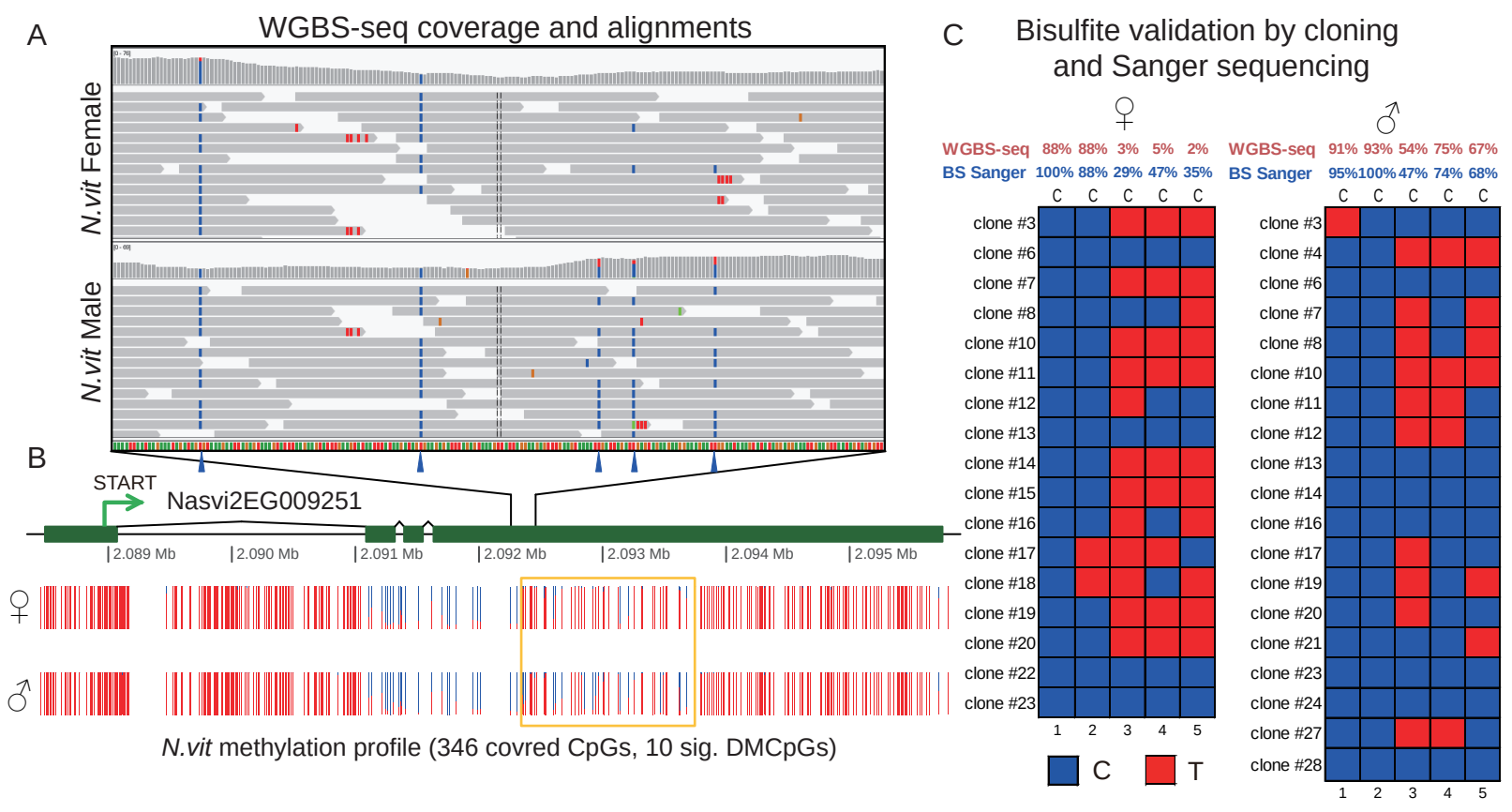
A
WGBS-seq coverage and alignments
N.vit Female
N.vit Male
B
START
Nasvi2EG009251
2.089 Mb
2.090 Mb
2.091 Mb
2.092 Mb
2.093 Mb
2.094 Mb
2.095 Mb
♀
♂
N.vit methylation profile (346 covred CpGs, 10 sig. DMCpGs)
C
Bisulfite validation by cloning and Sanger sequencing
♀
WGBS-seq 88% 88% 3% 5% 2%
BS Sanger 100% 88% 29% 47% 35%
C C C C C
clone #3
clone #6
clone #7
clone #8
clone #10
clone #11
clone #12
clone #13
clone #14
clone #15
clone #16
clone #17
clone #18
clone #19
clone #20
clone #22
clone #23
1 2 3 4 5
C
T
♂
WGBS-seq 91% 93% 54% 75% 67%
BS Sanger 95% 100% 47% 74% 68%
C C C C C
clone #3
clone #4
clone #6
clone #7
clone #8
clone #10
clone #11
clone #12
clone #13
clone #14
clone #16
clone #17
clone #19
clone #20
clone #21
clone #23
clone #24
clone #27
clone #28
1 2 3 4 5

Supporting Figure S9. Validation of CpG methylation status for candidate female-biased methylated gene Nasvi2EG007706 in *N. vitripennis*.

(A) IGV browser screenshot of *N. vitripennis* female (top) and male (bottom) WGBS-seq alignments in a 128 bp region in exon 4 of gene Nasvi2EG007706 on SCAFFOLD14, with 6 differentially methylated CpG sites pointed with blue arrows at the bottom. All 6 CpGs display a higher methylation level in females.

(B) Plots of the gene model, translation start site (on the - strand) and CpG methylation profile in both sexes for Nasvi2EG007706 from the WGBS-seq data. A vertical bar was drawn for each CpG at its position in the gene, color-coded by the methylation percentage in proportion to the bar length (blue: methylated Cs; red: non-methylated Cs that were converted to Ts). From this plot, Nasvi2EG007706 is methylated in both females and males, with the majority of the methylation within 5'-1kb coding region. 92 CpGs covered with a read depth of 6 or more were shown here, and 5 significantly differentially methylated between sexes (DMCpGs, within the orange box) are located at the 3'-boundary of the methylated CpGs cluster (the transcript is on the minus strand).

(C) Validation of the female-biased methylation by PyroMark assay. Raw pyrograms were shown for the methylation quantification of the 6 CpG sites shown in (A) for males and females from two independent biological replicates. There was no significant female-biased methylation percentage for all six sites. Therefore, the female-biased methylation for Nasvi2EG007706 was not confirmed in different biological replicates.

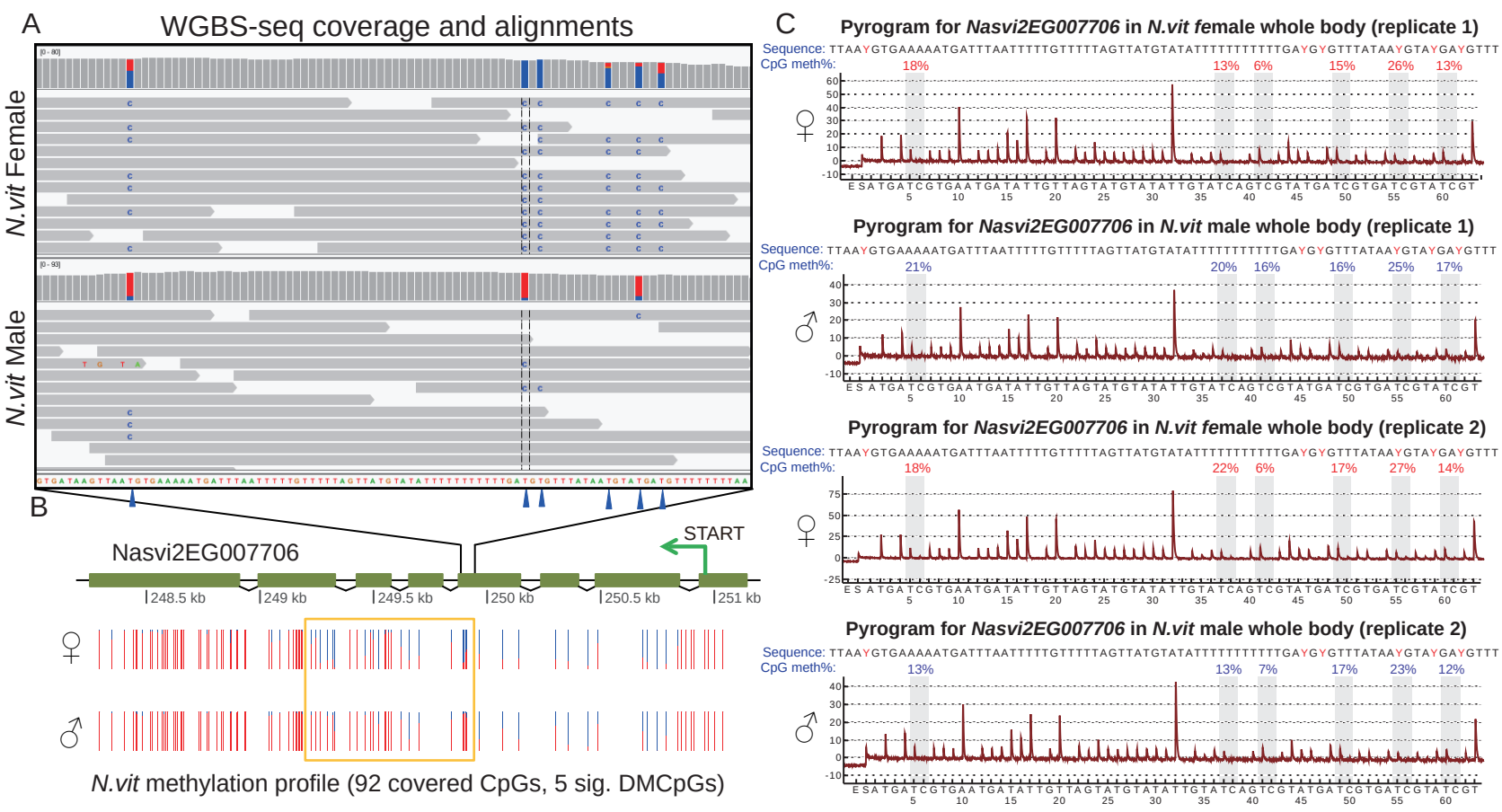
A
WGBS-seq coverage and alignments
N.vit Female
N.vit Male
B
Nasvi2EG007706
START
248.5 kb
249 kb
249.5 kb
250 kb
250.5 kb
251 kb
N.vit methylation profile (92 covered CpGs, 5 sig. DMCpGs)
C
Pyrogram for Nasvi2EG007706 in N.vit female whole body (replicate 1)
Sequence: TTAAYGTGAAAAATGATTTAATTTTTGTTTTTAGTTATGTATATTTTTTTTTTTTGAYGYGTTTATAAYGTAYGAYGTTT
CpG meth%: 18% 13% 6% 15% 26% 13%
Pyrogram for Nasvi2EG007706 in N.vit male whole body (replicate 1)
Sequence: TTAAYGTGAAAAATGATTTAATTTTTGTTTTTAGTTATGTATATTTTTTTTTTTTGAYGYGTTTATAAYGTAYGAYGTTT
CpG meth%: 21% 20% 16% 16% 25% 17%
Pyrogram for Nasvi2EG007706 in N.vit female whole body (replicate 2)
Sequence: TTAAYGTGAAAAATGATTTAATTTTTGTTTTTAGTTATGTATATTTTTTTTTTTTGAYGYGTTTATAAYGTAYGAYGTTT
CpG meth%: 18% 22% 6% 17% 27% 14%
Pyrogram for Nasvi2EG007706 in N.vit male whole body (replicate 2)
Sequence: TTAAYGTGAAAAATGATTTAATTTTTGTTTTTAGTTATGTATATTTTTTTTTTTTGAYGYGTTTATAAYGTAYGAYGTTT
CpG meth%: 13% 13% 7% 17% 23% 12%

Supporting Figure S10. Validation of CpG methylation status for candidate male-biased methylated gene Nasvi2EG002107 in *N. vitripennis*.

(A) IGV browser screenshot of *N. vitripennis* female (top) and male (bottom) WGBS-seq alignments in a 199 bp region in exon 11 of gene Nasvi2EG002107 on SCAFFOLD2, with 5 CpG sites pointed with blue arrows at the bottom. All 5 CpGs display higher methylation level in females.

(B) Plots of the gene model, translation start site and CpG methylation profile in both sexes for Nasvi2EG002107 from the WGBS-seq data. A vertical bar was drawn for each CpG at its position in the gene, color-coded by the methylation percentage in proportion to the bar length (blue: methylated Cs; red: non-methylated Cs that were converted to Ts). From this plot, Nasvi2EG002107 is methylated in both females and males, with the majority of the methylation within 5'-1kb coding region. 69 CpGs covered with 6 or more depth were shown here, and 5 significantly differentially methylated between sexes (DMCpGs, within the orange box) are located in the middle of the gene toward the 3'-boundary of the methylated CpGs cluster (the transcript is on the minus strand).

(C) Bisulfite sequencing verification results for the 5 CpGs sites shown in (A) using the cloning and Sanger sequencing method in both sexes from an independent biological replicate. The estimated methylation percentages at each CpG site from the WGBS-seq and single-gene bisulfite sequencing were shown on the top. At the 5 DMCpG sites, the female methylation level (45.4% on average) is not significantly higher than in the males (42%). Therefore, the female-biased methylation for Nasvi2EG002107 was not confirmed.

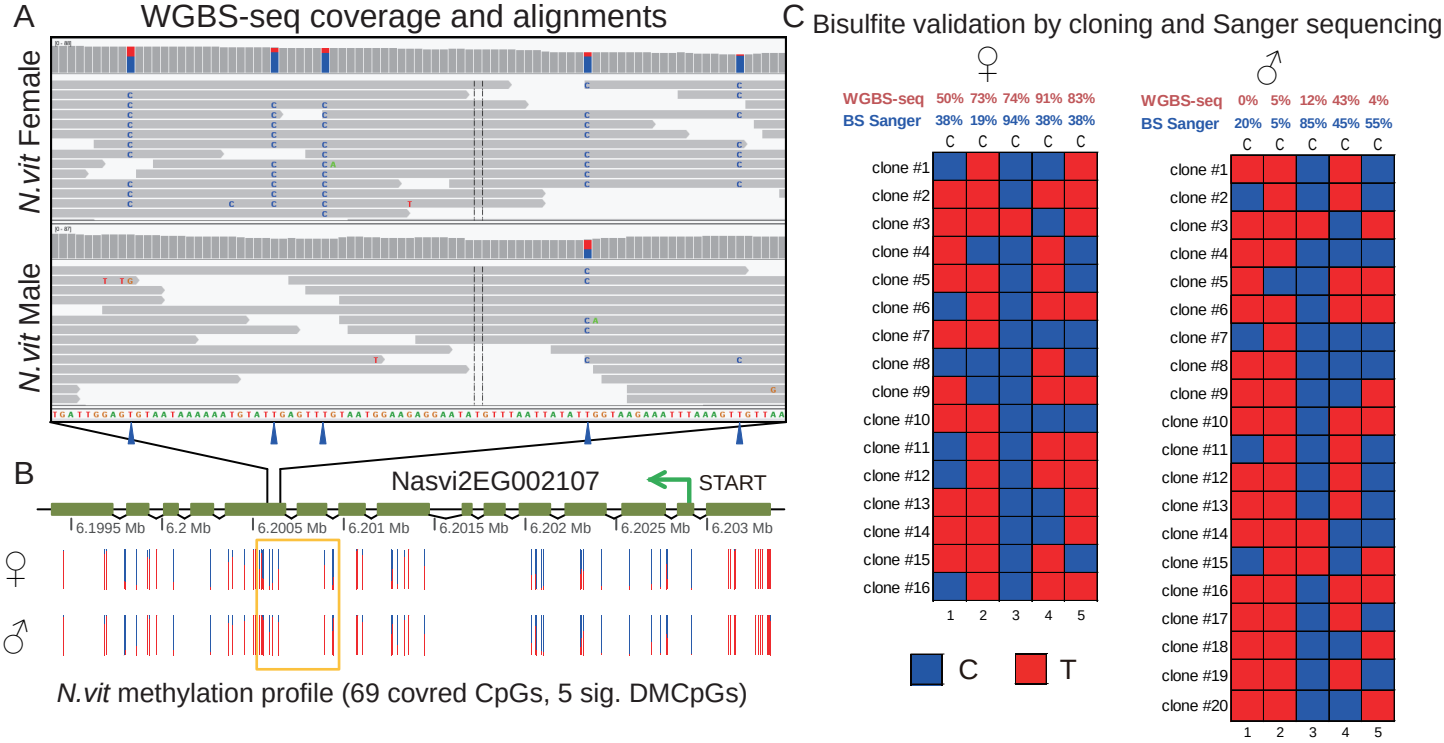
A
WGBS-seq coverage and alignments
N.vit Female
N.vit Male
B
Nasvi2EG002107
START
6.1995 Mb
6.2 Mb
6.2005 Mb
6.201 Mb
6.2015 Mb
6.202 Mb
6.2025 Mb
6.203 Mb
N.vit methylation profile (69 covred CpGs, 5 sig. DMCpGs)
C
Bisulfite validation by cloning and Sanger sequencing
WGBS-seq 50% 73% 74% 91% 83%
BS Sanger 38% 19% 94% 38% 38%
WGBS-seq 0% 5% 12% 43% 4%
BS Sanger 20% 5% 85% 45% 55%
clone #1
clone #2
clone #3
clone #4
clone #5
clone #6
clone #7
clone #8
clone #9
clone #10
clone #11
clone #12
clone #13
clone #14
clone #15
clone #16
clone #17
clone #18
clone #19
clone #20
1 2 3 4 5
C
T

Supporting Figure S11. Validation of CpG methylation status for candidate female-biased methylated gene Nasvi2EG008059 in *N. vitripennis*.

(A) IGV browser screenshot of *N. vitripennis* female (top) and male (bottom) WGBS-seq alignments in a 103 bp region in exon 3 of gene Nasvi2EG008059 on SCAFFOLD15, with 5 CpG sites pointed with blue arrows at the bottom. All 5 CpGs display higher methylation level in females.

(B) Plots of the gene model, translation start site and CpG methylation profile in both sexes for Nasvi2EG008059 from the WGBS-seq data. A vertical bar was drawn for each CpG at its position in the gene, color-coded by the methylation percentage in proportion to the bar length (blue: methylated Cs; red: non-methylated Cs that were converted to Ts). Another transcript, Nasvi2EG008060 (plotted in blue), is nested within intron 1 of Nasvi2EG008059. Nasvi2EG008060 is heavily methylated for the entire gene region. In the coding regions, Nasvi2EG008059 is methylated in females and non-methylated in males. 195 CpGs covered with 6 or more depth were shown here, and 5 significantly differentially methylated between sexes (DMCpGs, within the orange box) are located at the 3'-boundary of the methylated CpGs cluster.

(C) Bisulfite sequencing verification results for the 5 CpGs sites shown in (A) using the cloning and Sanger sequencing method in both sexes from an independent biological replicate. The estimated methylation percentages at each CpG site from the WGBS-seq and single-gene bisulfite sequencing were shown on the top. At the 5 DMCpGs, female methylation profile matched well for most sites, but in males they display much higher percentage of methylation (67% on average) than in the WGBS-seq data (11.4% on average) and the female methylation is not significantly higher than in male. Therefore, the female-biased methylation for Nasvi2EG008059 was not confirmed.

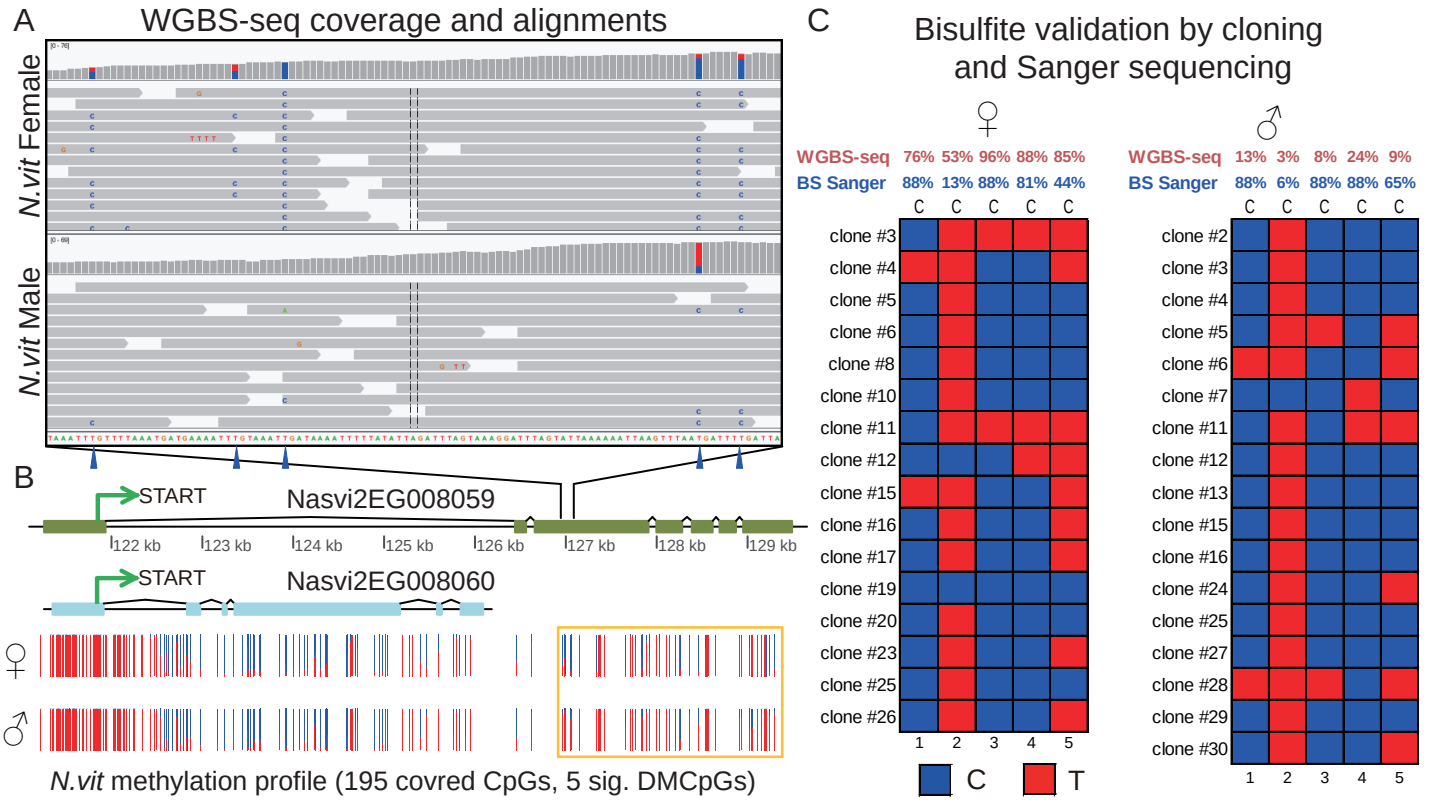
A
WGBS-seq coverage and alignments
N.vit Female
N.vit Male
B
START
Nasvi2EG008059
122 kb
123 kb
124 kb
125 kb
126 kb
127 kb
128 kb
129 kb
START
Nasvi2EG008060
♀
♂
N.vit methylation profile (195 covred CpGs, 5 sig. DMCpGs)
C
Bisulfite validation by cloning and Sanger sequencing
♀
WGBS-seq 76% 53% 96% 88% 85%
BS Sanger 88% 13% 88% 81% 44%
C C C C C
clone #3
clone #4
clone #5
clone #6
clone #8
clone #10
clone #11
clone #12
clone #15
clone #16
clone #17
clone #19
clone #20
clone #23
clone #25
clone #26
1 2 3 4 5
C
T
♂
WGBS-seq 13% 3% 8% 24% 9%
BS Sanger 88% 6% 88% 88% 65%
C C C C C
clone #2
clone #3
clone #4
clone #5
clone #6
clone #7
clone #11
clone #12
clone #13
clone #15
clone #16
clone #24
clone #25
clone #27
clone #28
clone #29
clone #30
1 2 3 4 5

Supporting Figure S12. DNA methylation correlation between *N. vitripennis* and *N. girault*i female and male adults.

Pairwise scatterplots of the DNA methylation percentage at 78,494 methylated CpGs sites among *N. vitripennis* and *N. girault*i adult females and males (***bottom-left***), color-coded by the point density. Plotted in the diagonal panels are the histograms of methylation percentages. Spearman correlation coefficients are shown in the top-right panels, with text size in proportion to the value.

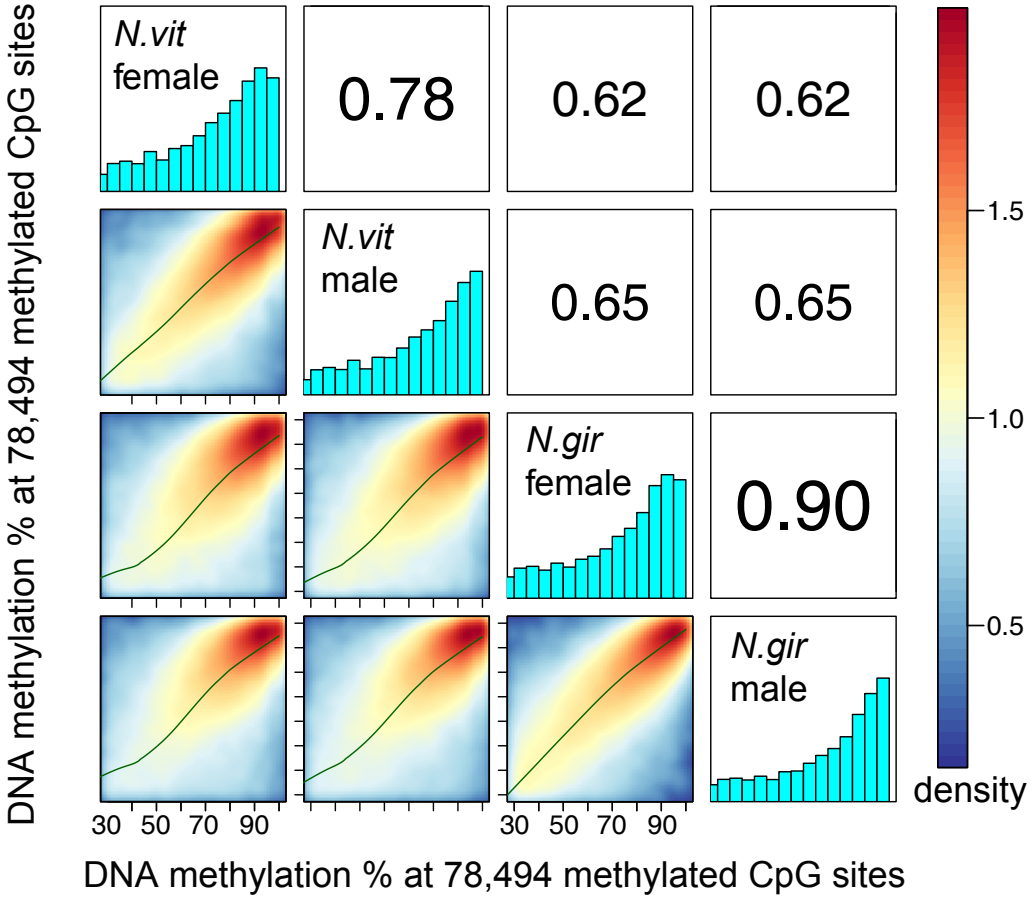

Supporting Figure S13. Validation of *N. giraulti* -biased methylated gene Nasvi2EG013110 in *N. vitripennis* and *N. giraulti* using the PyroMark assay.

(A) IGV browser screenshot of WGBS-seq alignments for a 68 bp region in Nasvi2EG013110 on SCAFFOLD34 for *N. vitripennis* female, *N. vitripennis* male, *N. giraulti* female and *N. giraulti* male (from top to bottom), showing 6 CpG sites (blue arrows at the bottom) which are only methylated in *N. giraulti*. In the coverage bar plot on the top panel, the blue portion strands for methylated Cs that remain Cs and the red portion strands for non-methylated Cs which are converted to Ts.

(B) Plots of the gene model, translation start site and CpG methylation profile in females and males of both species for Nasvi2EG013110 from the WGBS-seq data. A vertical bar was drawn for each CpG at its position in the gene, color-coded by the methylation percentage in proportion to the bar length (blue: methylated Cs; red: non-methylated Cs that were converted to Ts). Among 206 CpGs covered with a depth of 6 or more in all four samples, 46 (within the orange box) displayed significantly different methylation between *N. vitripennis* and *N. giraulti*.

(C) Validation of the *N. giraulti*-biased methylation by PyroMark assay in females and males of both species. Raw pyrograms were shown for the methylation quantification of the 6 CpG sites shown in (A). Zero methylation was observed for *N. vitripennis* samples and 70-100% methylation in *N. giraulti*. The assays were performed with two technical replicates using the same primer set and in the same batch for all four samples.

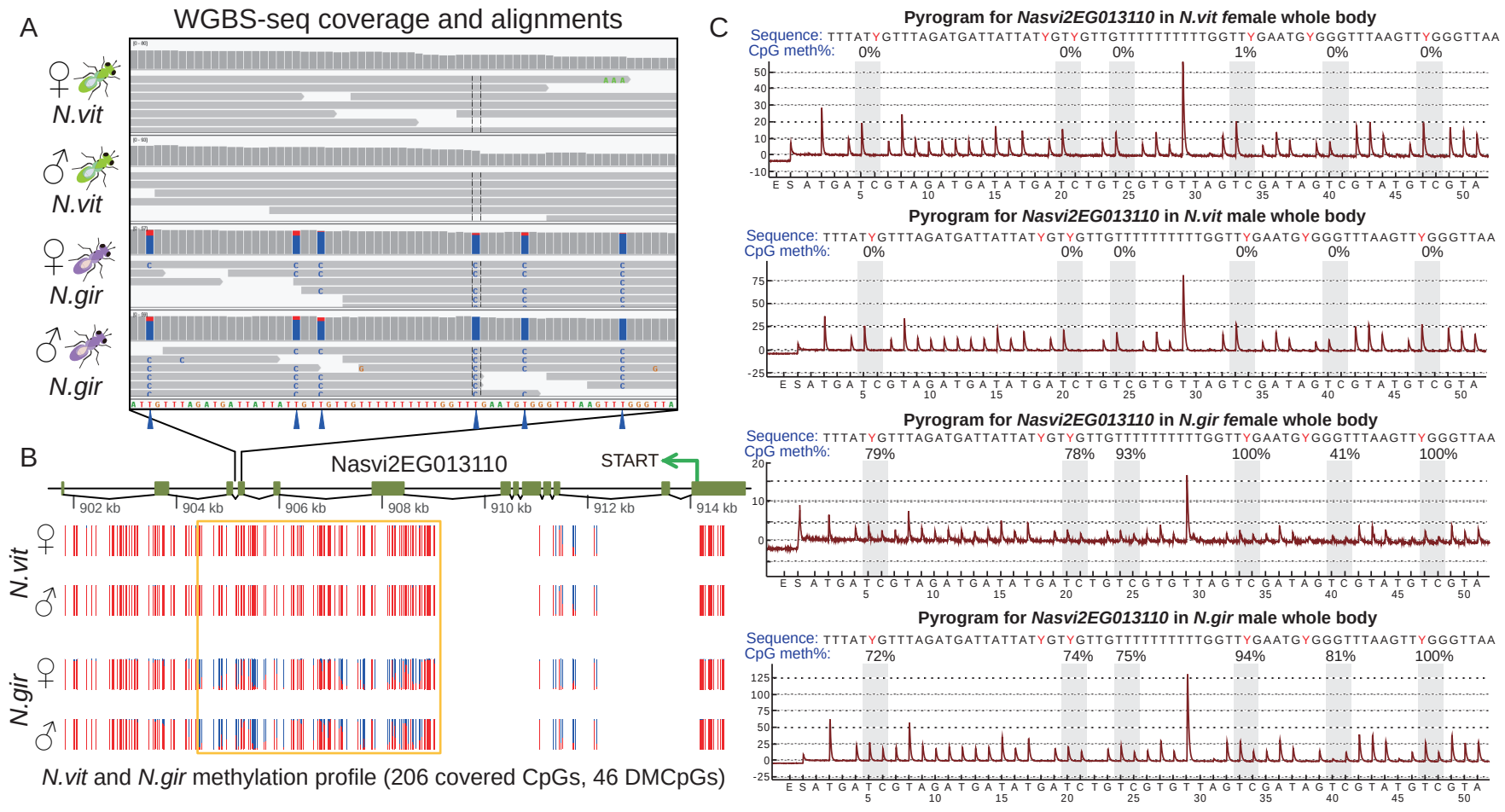

N.vit and *N.gir* methylation profile (206 covered CpGs, 46 DMCpGs)

Supporting Figure S14. Validation of *N. vitripennis*-biased methylated gene Nasvi2EG030779 in *N. vitripennis* and *N. giraulti* using the PyroMark assay.

(A) IGV browser screenshot of WGBS-seq alignments for a 135 bp region in Nasvi2EG030779 on SCAFFOLD682 for *N. vitripennis* female, *N. vitripennis* male, *N. giraulti* female and *N. giraulti* male (from top to bottom), showing 6 CpG sites (blue arrows at the bottom) which are only methylated in *N. vitripennis* as well as one A/G SNP (orange arrow at the bottom) between *N. vitripennis* and *N. giraulti*.

(B) Plots of the gene model, translation start site and CpG methylation profile in females and males of both species for Nasvi2EG030779 from the WGBS-seq data. A vertical bar was drawn for each CpG at its position in the gene, color-coded by the methylation percentage in proportion to the bar length (blue: methylated Cs; red: non-methylated Cs that were converted to Ts). Among 131 CpGs covered with a depth of 6 or more in all four samples, 48 (within the orange box) displayed significantly different methylation between *N. vitripennis* and *N. giraulti*.

(C) Validation of the *N. vitripennis*-biased methylation by PyroMark assay in females and males of both species. Raw pyrograms were shown for the methylation quantification of the 6 CpG sites shown in (A). Zero methylation was observed for *N. giraulti* samples and 70-100% methylation in *N. vitripennis*. At the A/G SNP position, *N. vitripennis* has the A allele *N. giraulti* has the G allele, which is consistent with the SNP genotypes. The assays were performed with two technical replicates using the same primer set and in the same batch for all four samples.

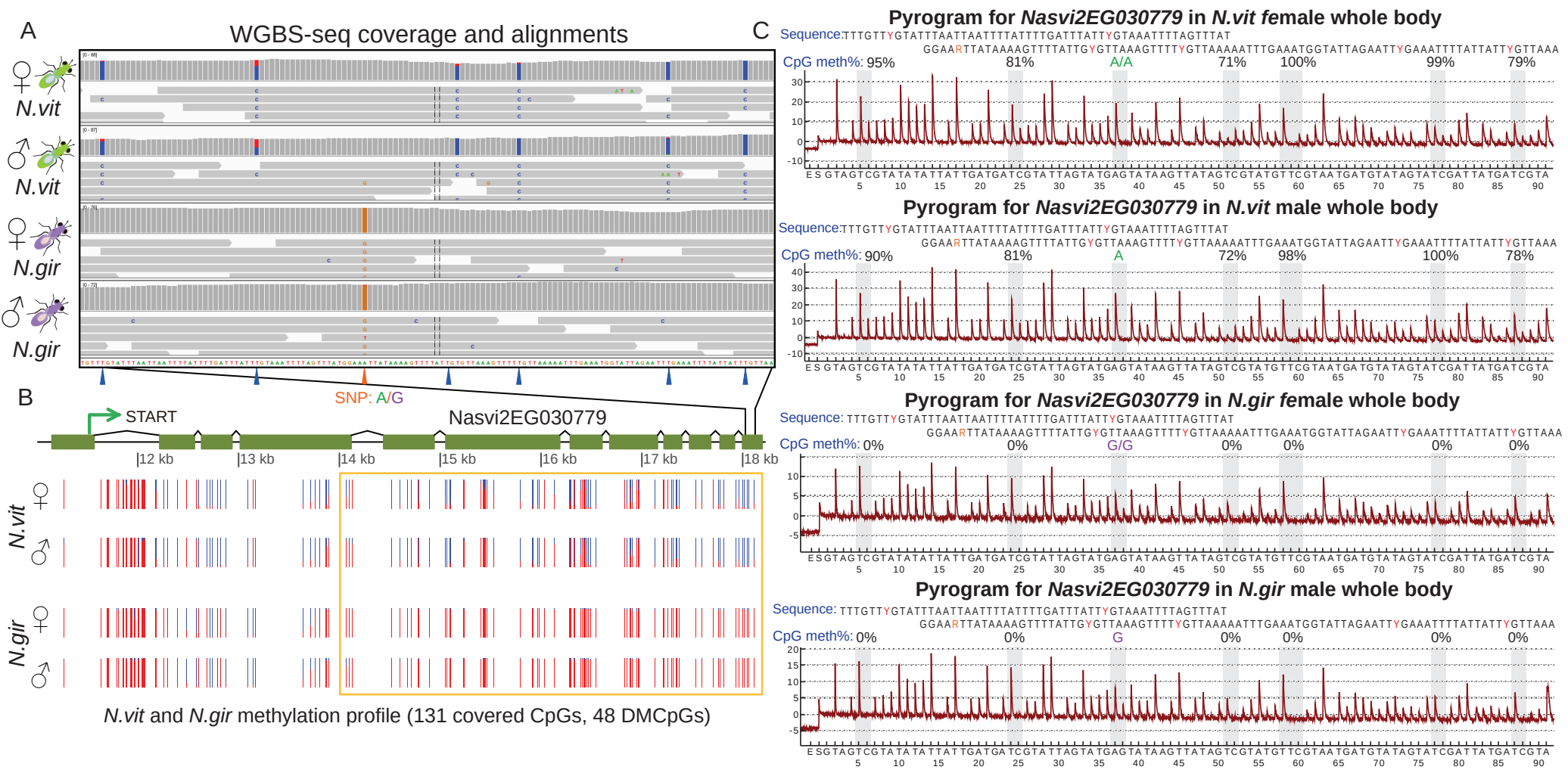

N.vit and *N.gir* methylation profile (131 covered CpGs, 48 DMCpGs)

Supporting Figure S15. Validation of *N. vitripennis*-biased methylated gene Nasvi2EG013343 in *N. vitripennis* and *N. giraulti* using the PyroMark assay.

(A) IGV browser screenshot of WGBS-seq alignments for a 98 bp region in Nasvi2EG013343 on SCAFFOLD35 for *N. vitripennis* female, *N. vitripennis* male, *N. giraulti* female and *N. giraulti* male (from top to bottom), showing 6 CpG sites (blue arrows at the bottom) which are only methylated in *N. vitripennis*.

(B) Plots of the gene model, translation start site and CpG methylation profile in females and males of both species for Nasvi2EG013343 from the WGBS-seq data. A vertical bar was drawn for each CpG at its position in the gene, color-coded by the methylation percentage in proportion to the bar length (blue: methylated Cs; red: non-methylated Cs that were converted to Ts). Among 108 CpGs covered with a depth of 6 or more in all four samples, 29 (within the orange box) displayed significantly different methylation between *N. vitripennis* and *N. giraulti*.

(C) Validation of the *N. vitripennis*-biased methylation by PyroMark assay in females and males of both species. Raw pyrograms were shown for the methylation quantification of the 6 CpG sites shown in (A). Zero methylation was observed for *N. giraulti* samples and 70-100% methylation in *N. vitripennis*. The assays were performed with two technical replicates using the same primer set and in the same batch for all four samples.

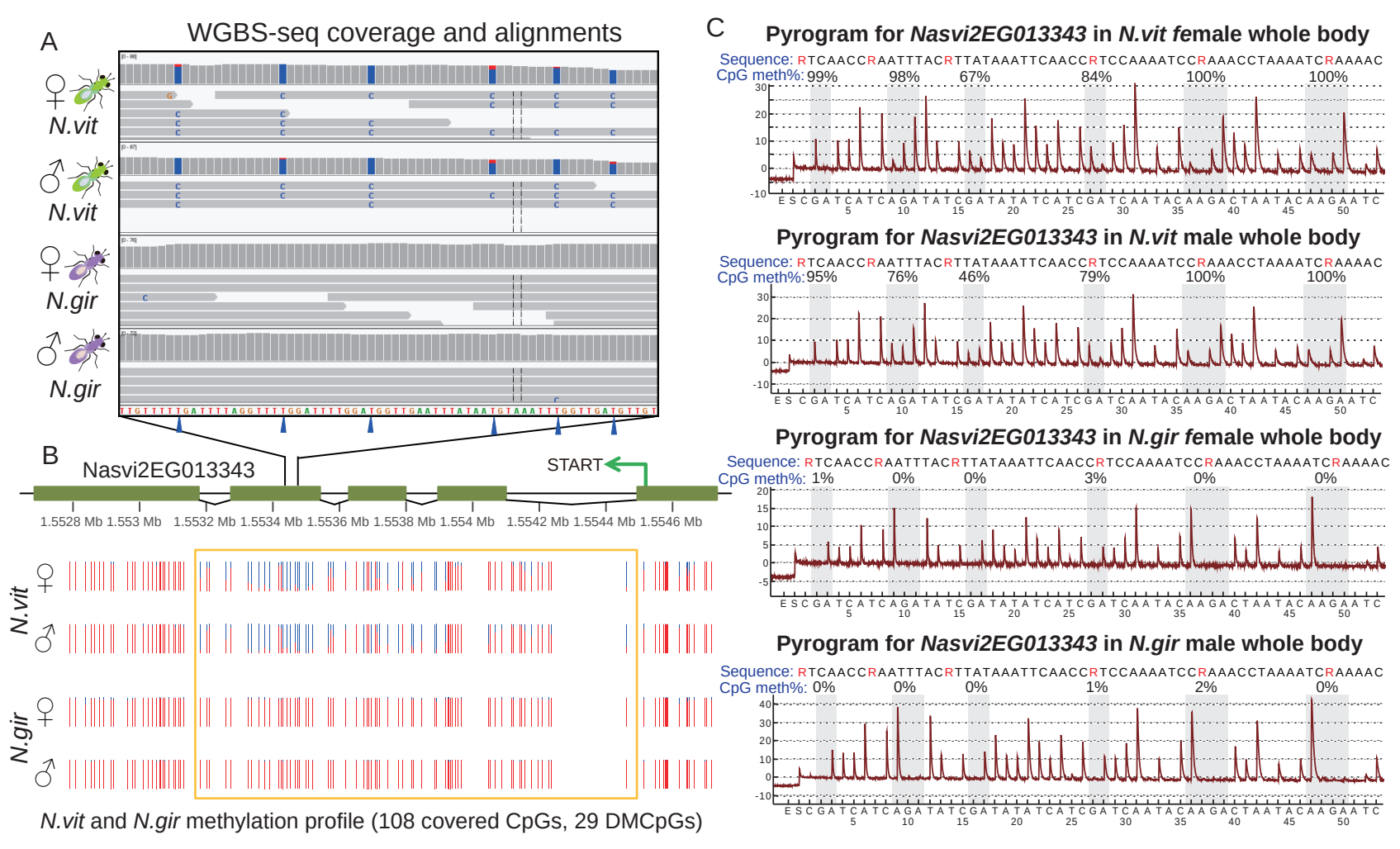

N.vit and *N.gir* methylation profile (108 covered CpGs, 29 DMCpGs)

Supporting Figure S16. Validation of the *N. vitripennis*-biased methylated gene Nasvi2EG017109 in *N. vitripennis* and *N. giraulti* using the PyroMark assay.

(A) IGV browser screenshot of WGBS-seq alignments for a 117 bp region in Nasvi2EG017109 on SCAFFOLD69 for *N. vitripennis* female, *N. vitripennis* male, *N. giraulti* female and *N. giraulti* male (from top to bottom), showing 4 CpG sites (blue arrows at the bottom) which are only methylated in *N. vitripennis* as well as three SNPs (orange arrow at the bottom) between *N. vitripennis* and *N. giraulti*. The SNP alleles are G/T, A/T and A/T from left to right (*N. vitripennis* first).

(B) Plots of the gene model, translation start site and CpG methylation profile in females and males of both species for Nasvi2EG017109 from the WGBS-seq data. A vertical bar was drawn for each CpG at its position in the gene, color-coded by the methylation percentage in proportion to the bar length (blue: methylated Cs; red: non-methylated Cs that were converted to Ts). Among 39 CpGs covered with a depth of 6 or more in all four samples, 17 (within the orange box) displayed significantly different methylation between *N. vitripennis* and *N. giraulti*.

(C) Validation of the *N. vitripennis*-biased methylation by PyroMark assay in females and males of both species. Raw pyrograms were shown for the methylation quantification of the 4 CpG sites shown in (A). Less than 20% methylation was observed for *N. giraulti* samples and 70-100% methylation in *N. vitripennis*. All three SNPs are consistent with the correct genotypes. The assays were performed with two technical replicates using the same primer set and in the same batch for all four samples.

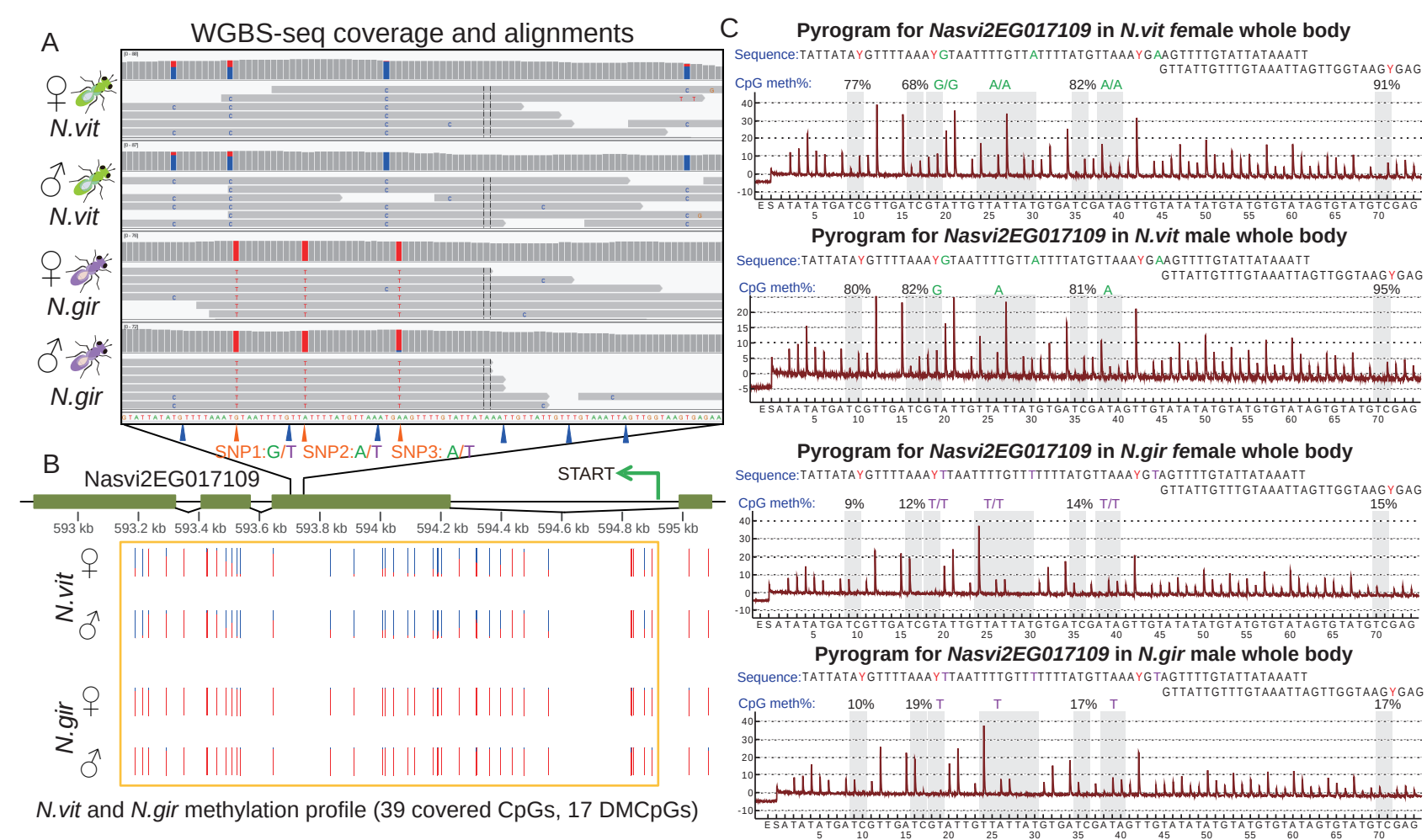

N.vit and *N.gir* methylation profile (39 covered CpGs, 17 DMCpGs)

Supporting Figure S17. Validation of *N. vitripennis*-biased methylated gene Nasvi2EG028410 in *N. vitripennis* and *N. giraulti* using the PyroMark assay.

(A) IGV browser screenshot of WGBS-seq alignments for a 11bp region in Nasvi2EG028410 on SCAFFOLD418 for *N. vitripennis* female, *N. vitripennis* male, *N. giraulti* female and *N. giraulti* male (from top to bottom), showing 5 CpG sites (blue arrows at the bottom) which are only methylated in *N. vitripennis*.

(B) Plots of the gene model, translation start site and CpG methylation profile in females and males of both species for Nasvi2EG028410 from the WGBS-seq data. A vertical bar was drawn for each CpG at its position in the gene, color-coded by the methylation percentage in proportion to the bar length (blue: methylated Cs; red: non-methylated Cs that were converted to Ts). Among 172 CpGs covered with a read depth of 6 or more in all four samples, 25 (within the orange box) displayed significantly different methylation between *N. vitripennis* and *N. giraulti*.

(C) Validation of the *N. vitripennis*-biased methylation by PyroMark assay in females and males of both species. Raw pyrograms were shown for the methylation quantification of the 5 CpG sites shown in (A). Less than 10% methylation was observed for *N. giraulti* samples and 50-100% methylation in *N. vitripennis*. The assays were performed with two technical replicates using the same primer set and in the same batch for all four samples.

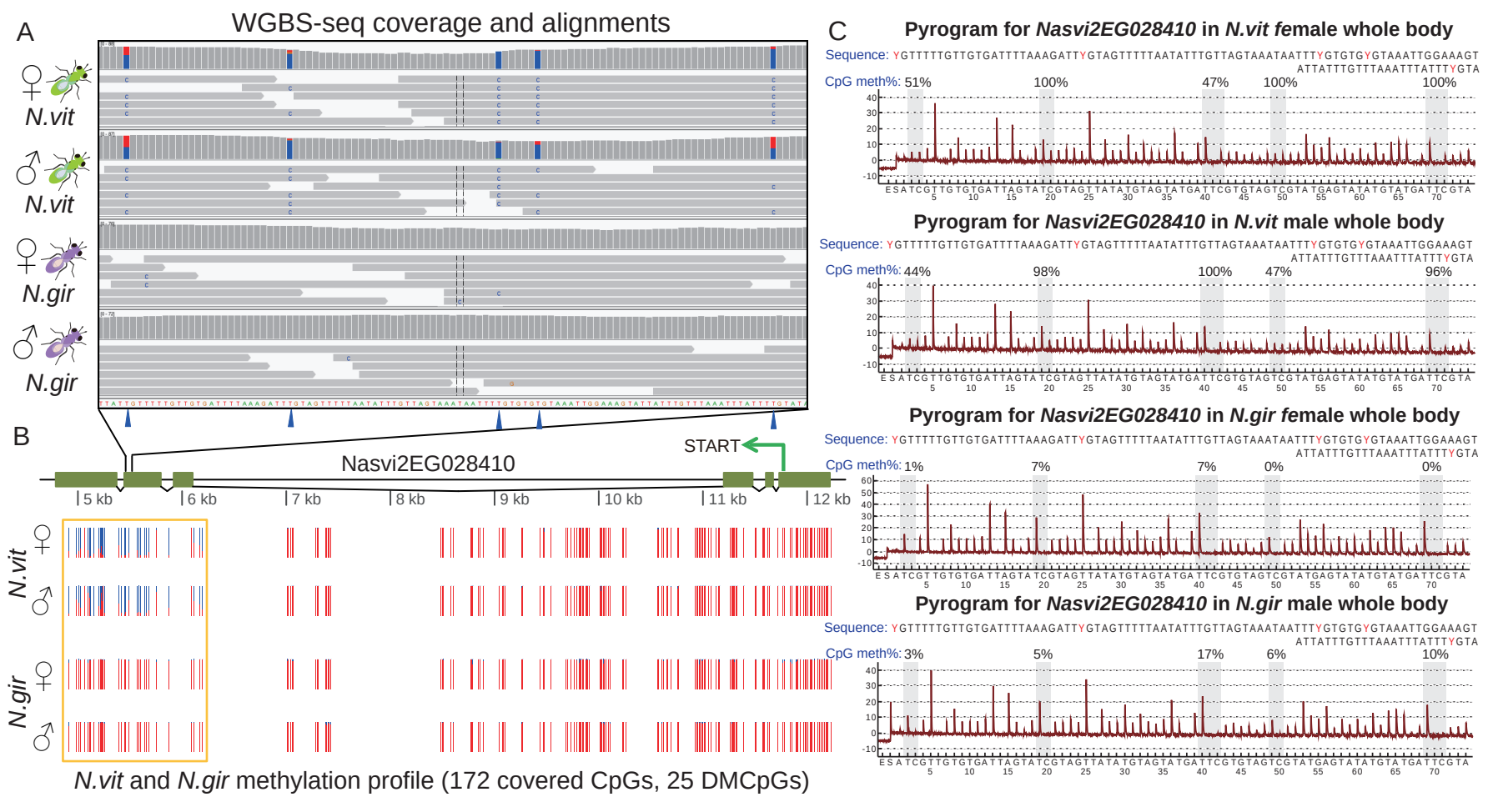

N.vit and *N.gir* methylation profile (172 covered CpGs, 25 DMCpGs)

Supporting Figure S18. Validation of *N. giraulti*-biased mehylated gene Nasvi2EG008123 in *N. vitripennis* and *N. giraulti* using the PyroMark assay.

(A) IGV browser screenshot of WGBS-seq alignments for a 50 bp region in Nasvi2EG008123 on SCAFFOLD15 for *N. vitripennis* female, *N. vitripennis* male, *N. giraulti* female and *N. giraulti* male (from top to bottom), showing 4 CpG sites (blue arrows at the bottom) which are only methylated in *N. giraulti*.

(B) Plots of the gene model, translation start site and CpG methylation profile in females and males of both species for Nasvi2EG008123 from the WGBS-seq data. A vertical bar was drawn for each CpG at its position in the gene, color-coded by the methylation percentage in proportion to the bar length (blue: methylated Cs; red: non-methylated Cs that were converted to Ts). Among 31 CpGs covered with a read depth of 6 or more in all four samples, 19 (within the orange box) displayed significantly different methylation between *N. vitripennis* and *N. giraulti*.

(C) Validation of the *N. giraulti*-biased methylation by PyroMark assay in females and males of both species. Raw pyrograms were shown for the methylation quantification of the 4 CpG sites shown in (A). Very low methylation level was observed for *N. vitripennis* samples and 63-95% methylation in *N. giraulti*. The assays were performed with two technical replicates using the same primer set and in the same batch for all four samples.

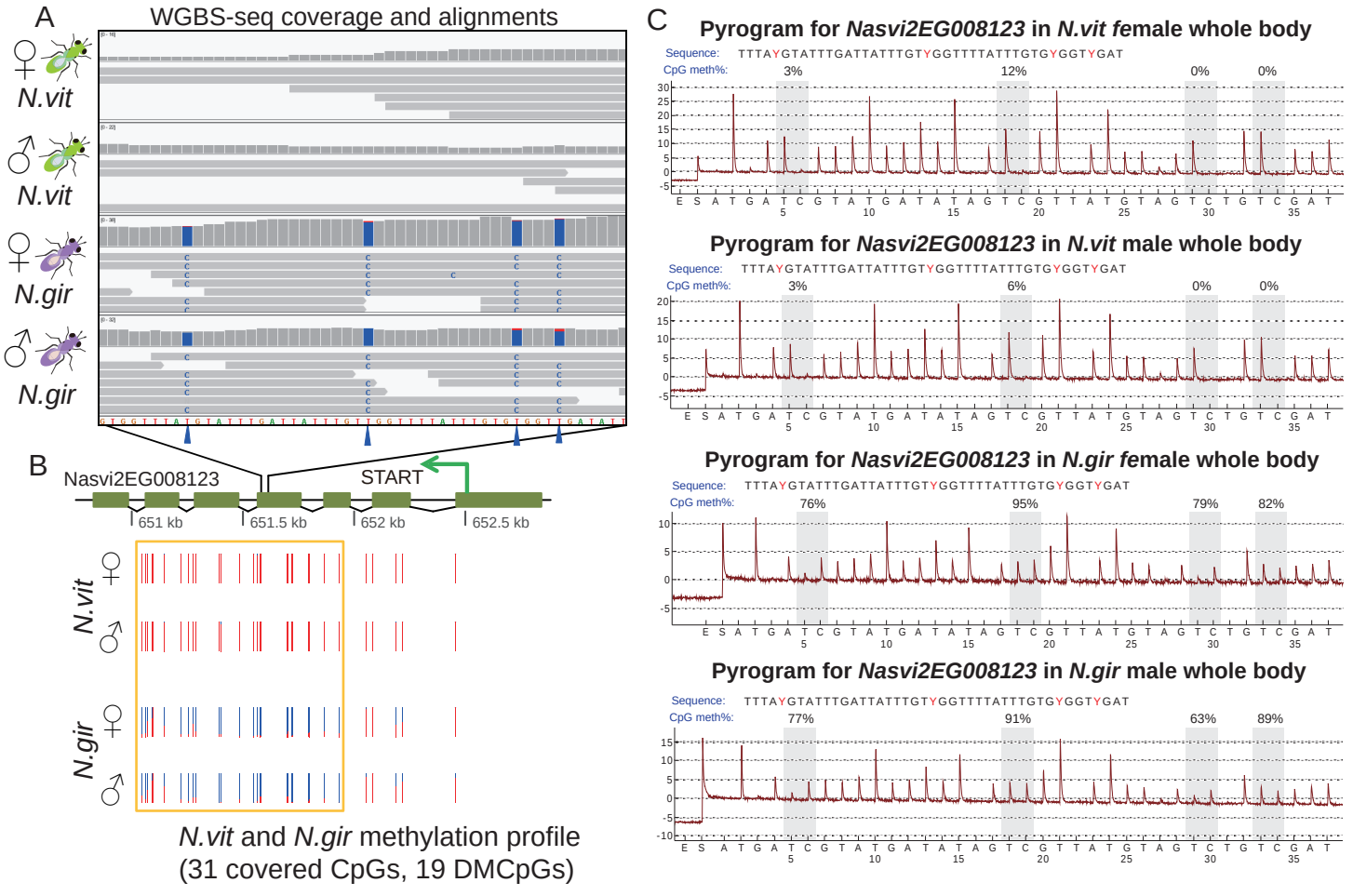
A
WGBS-seq coverage and alignments
N.vit
N.vit
N.gir
N.gir
B
Nasvi2EG008123
START
651 kb
651.5 kb
652 kb
652.5 kb
N.vit
N.gir
N.vit and N.gir methylation profile
(31 covered CpGs, 19 DMCpGs)
C
Pyrogram for Nasvi2EG008123 in N.vit female whole body
Sequence: TTTAYGTATTTGATTATTTGTYGGTTTTATTTGTGYGGTYGAT
CpG meth%: 3% 12% 0% 0%
Pyrogram for Nasvi2EG008123 in N.vit male whole body
Sequence: TTTAYGTATTTGATTATTTGTYGGTTTTATTTGTGYGGTYGAT
CpG meth%: 3% 6% 0% 0%
Pyrogram for Nasvi2EG008123 in N.gir female whole body
Sequence: TTTAYGTATTTGATTATTTGTYGGTTTTATTTGTGYGGTYGAT
CpG meth%: 76% 95% 79% 82%
Pyrogram for Nasvi2EG008123 in N.gir male whole body
Sequence: TTTAYGTATTTGATTATTTGTYGGTTTTATTTGTGYGGTYGAT
CpG meth%: 77% 91% 63% 89%

Supporting Figure S19. Methylation status and expression fold differences for sex-biased genes.

Boxplot of expression fold differences (log_{10} scale on *y*-axis) for methylated (blue) and non-methylated (red) male-biased (MB) and female-biased (FB) genes in whole-body and head samples. Statistical significance was calculated by Mann-Whitney U Test (**:*P*-value < 0.01; ***: *P*-value < 0.001).

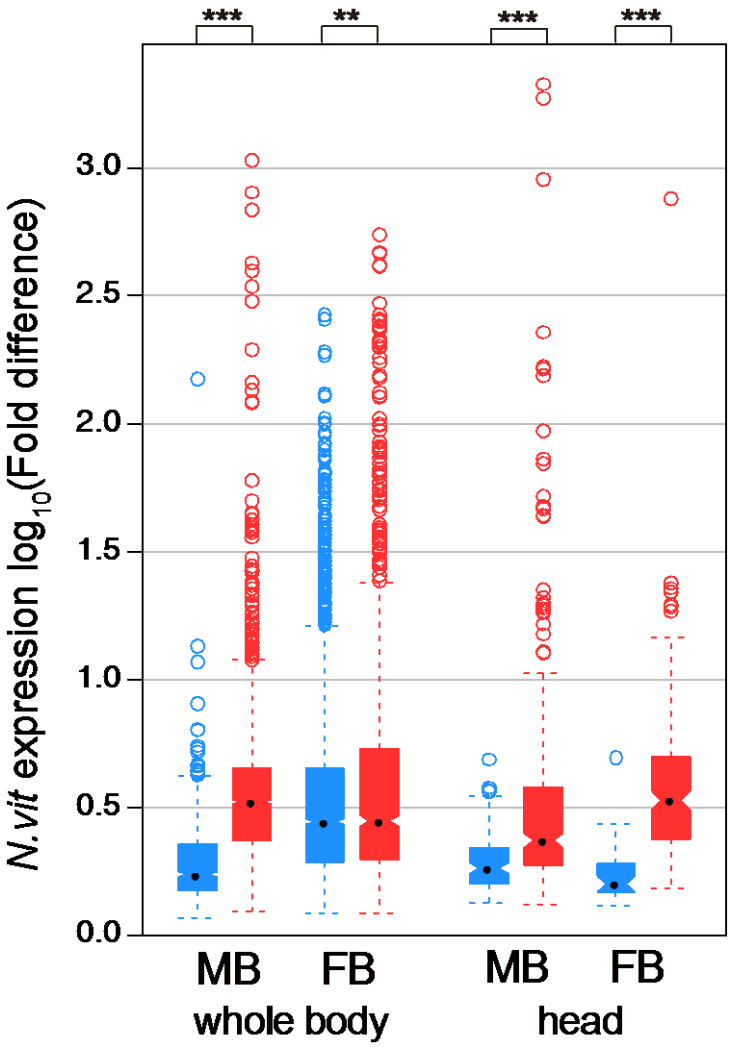

Supporting Figure S20. Degree of sex-biased expression and expression variability for methylated and non-methylated genes.

Scatterplot of expression CV across five developmental stages on the *x*-axis against log2 fold differences between the two sexes for male-biased non-methylated genes (upper left panel), female-biased non-methylated genes (upper right panel), male-biased methylated genes (lower left panel) and female-biased methylated genes (lower right panel).

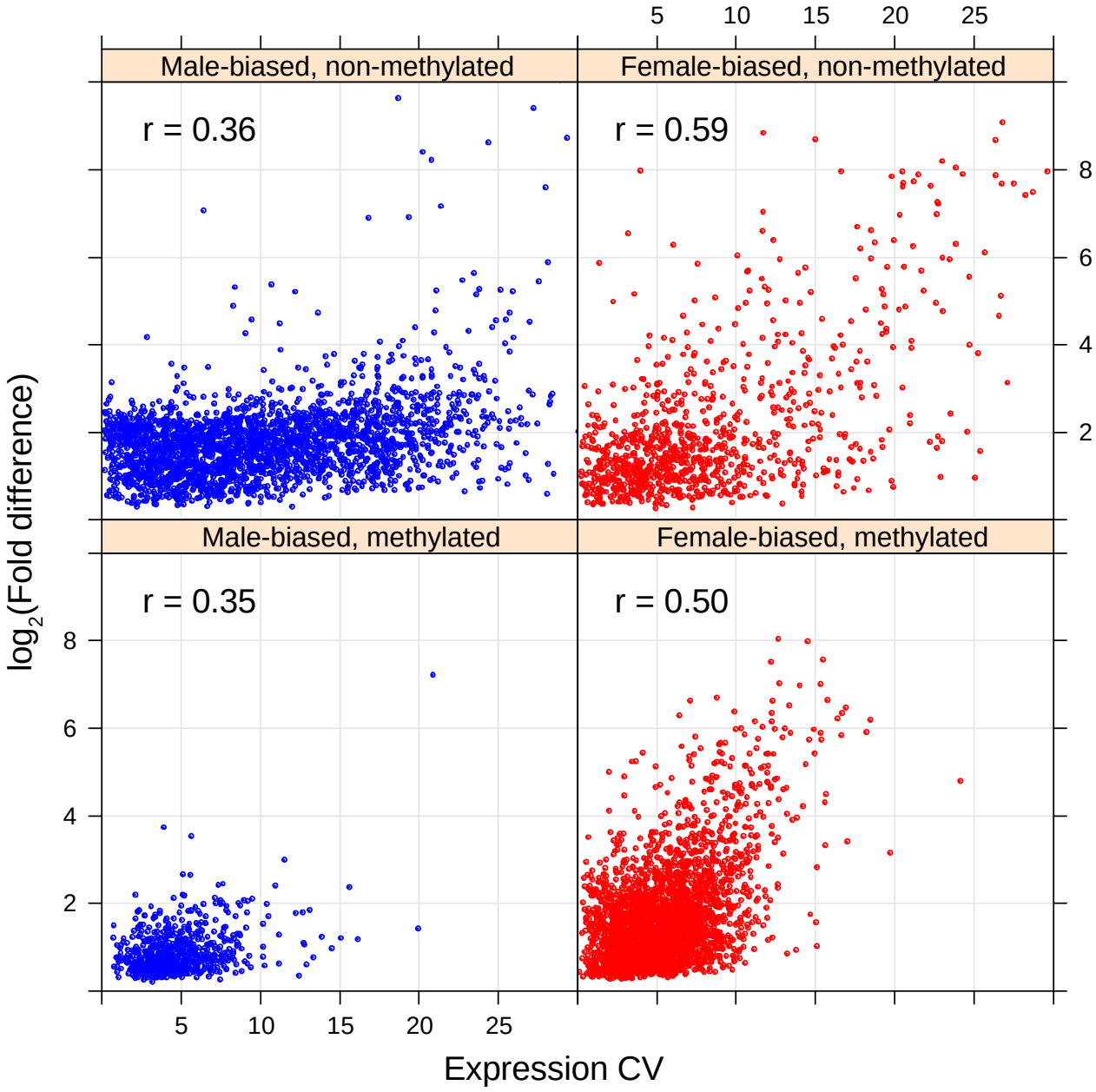

Supporting Figure S21. dN/dS ratios for sex-biased, sex-specific and unbiased genes.

Boxplot of dN/dS ratios for genes in the following sex-biased expression categories: MB: male-biased but not male-specific; FB: female-biased but not female-specific; UB: unbiased genes; MS: male-specific; FS: female-specific. Methylated (blue) and non-methylated genes (red) for all categories combined were also plotted.

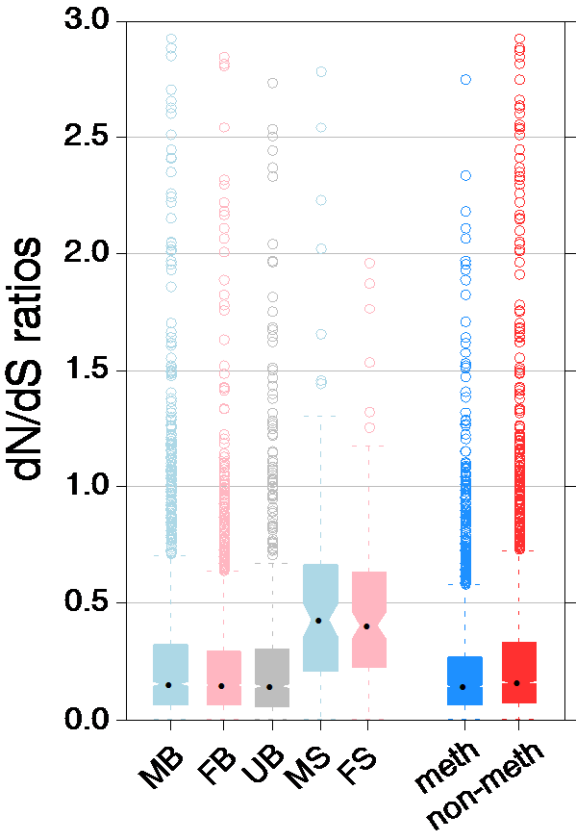

Supporting Figure S22. Negative correlation between expression breadth (number of expressed stages) and rate of evolution for female-biased and unbiased vs. male-biased genes. Boxplot of nucleotide divergence in coding regions between *N. vitripennis* and *N. giraulti* for female-biased and unbiased genes (pink, left panel) and male-biased genes (blue, right panel) in different express breadth categories (number of expressed developmental stages).

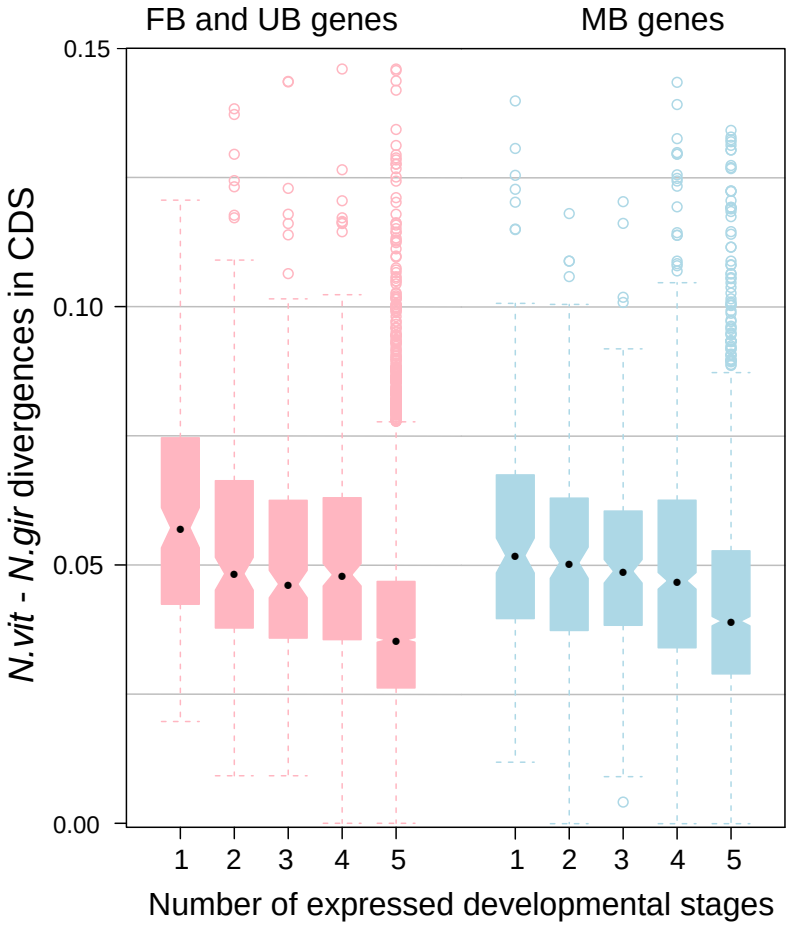

Supplemental Figure S23. Correlation between expression breadth (number of expressed stages) and dN/dS ratios for female-biased and unbiased genes combined.

Boxplot of dN/dS ratios for female-biased and unbiased genes in different express breadth categories (number of expressed developmental stages).

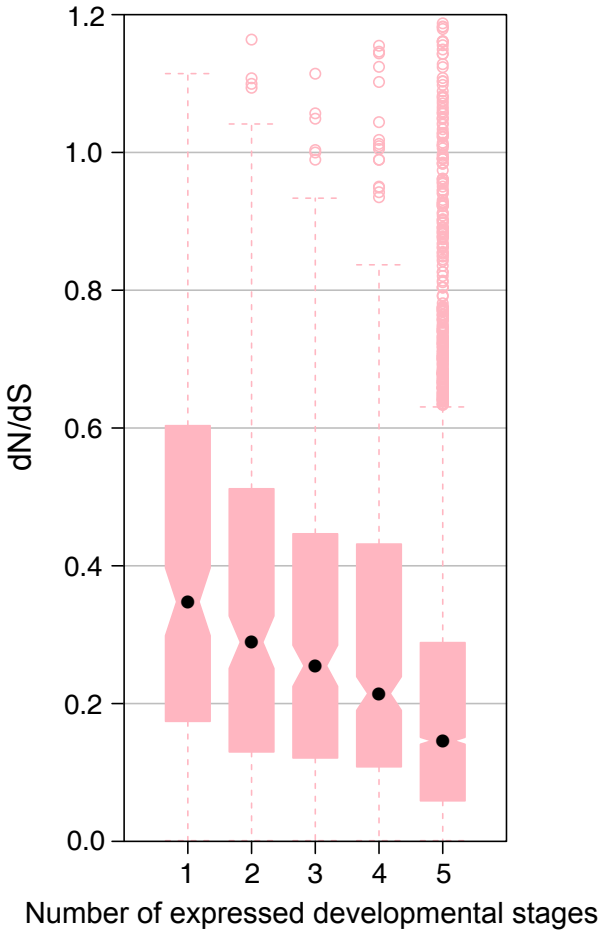

Supporting Figure S24 Chromosome location of sex-biased genes.

In each sub figure, plotted in the top panel is the genetic distance (cM) in black and local recombination intensity (cM/Mb) in red along *Nasonia* chromosomes. A green bar at mark positions was drawn at the bottom of the graph to demonstrate local marker density. Plotted in the bottom panel are the fold differences of male-biased (MB), female-biased (FB), male-specific (MS), female-specific (FS) and unbiased genes (UB). The pericentromeric with no recombination was labeled by a yellow box.

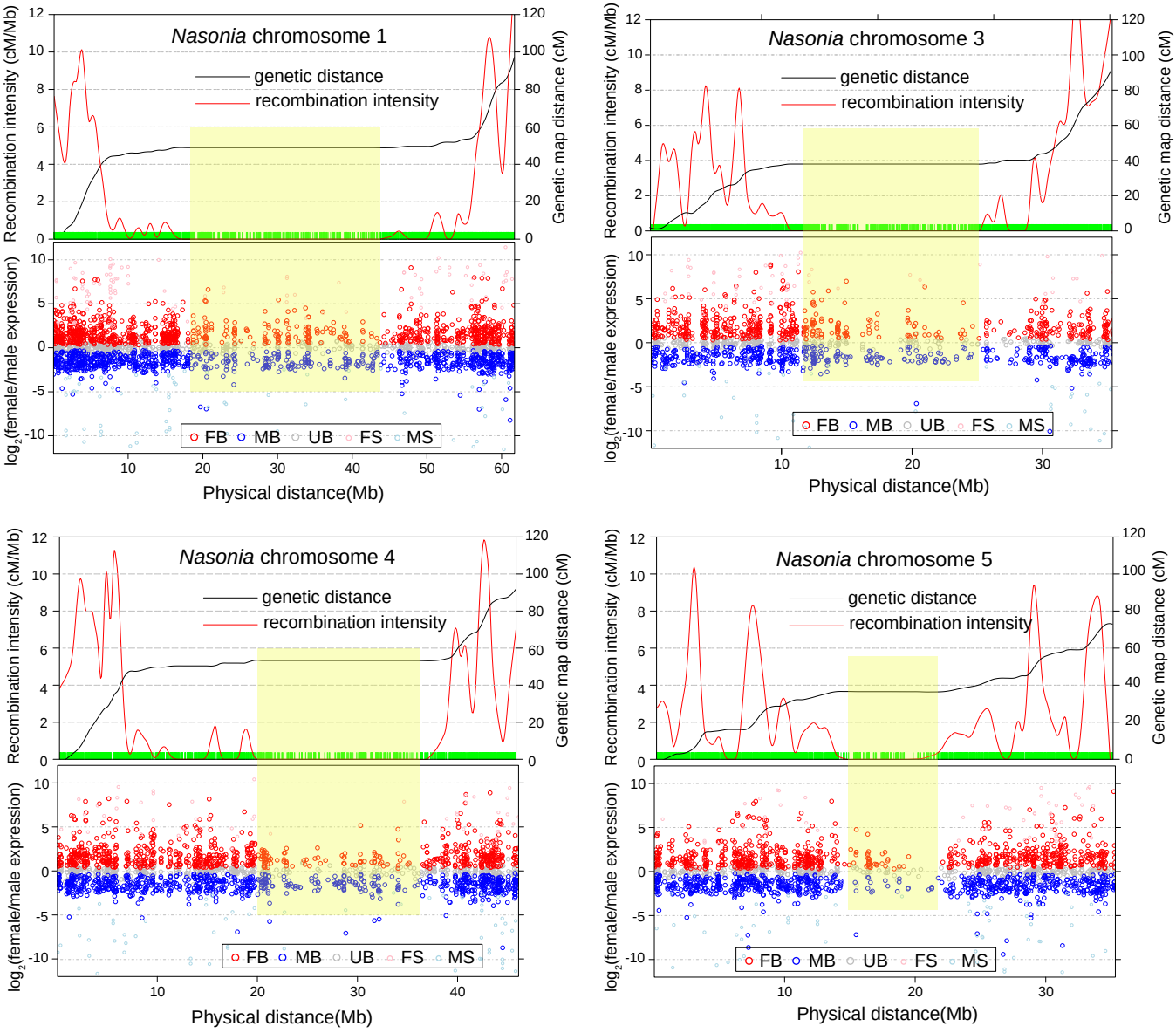

Supporting Figure S25. Recombination intensity for sex-biased genes.

Boxplot of local recombination intensity (cM/Mb) for genes in the following sex-biased expression categories: MB: male-biased but not male-specific; FB: female-biased but not female-specific; UB: unbiased genes; MS: male-specific; FS: female-specific. The left panel is for all genes and the right panel is for non-methylated genes only. Plotted in the middle panel is for methylated (blue) and non-methylated genes (red) for all categories combined. Statistical significance was calculated by Mann-Whitney U Test (ns: *P*-value > 0.05; *: *P*-value < 0.05; **: *P*-value < 0.01; ***: *P*-value < 0.001).

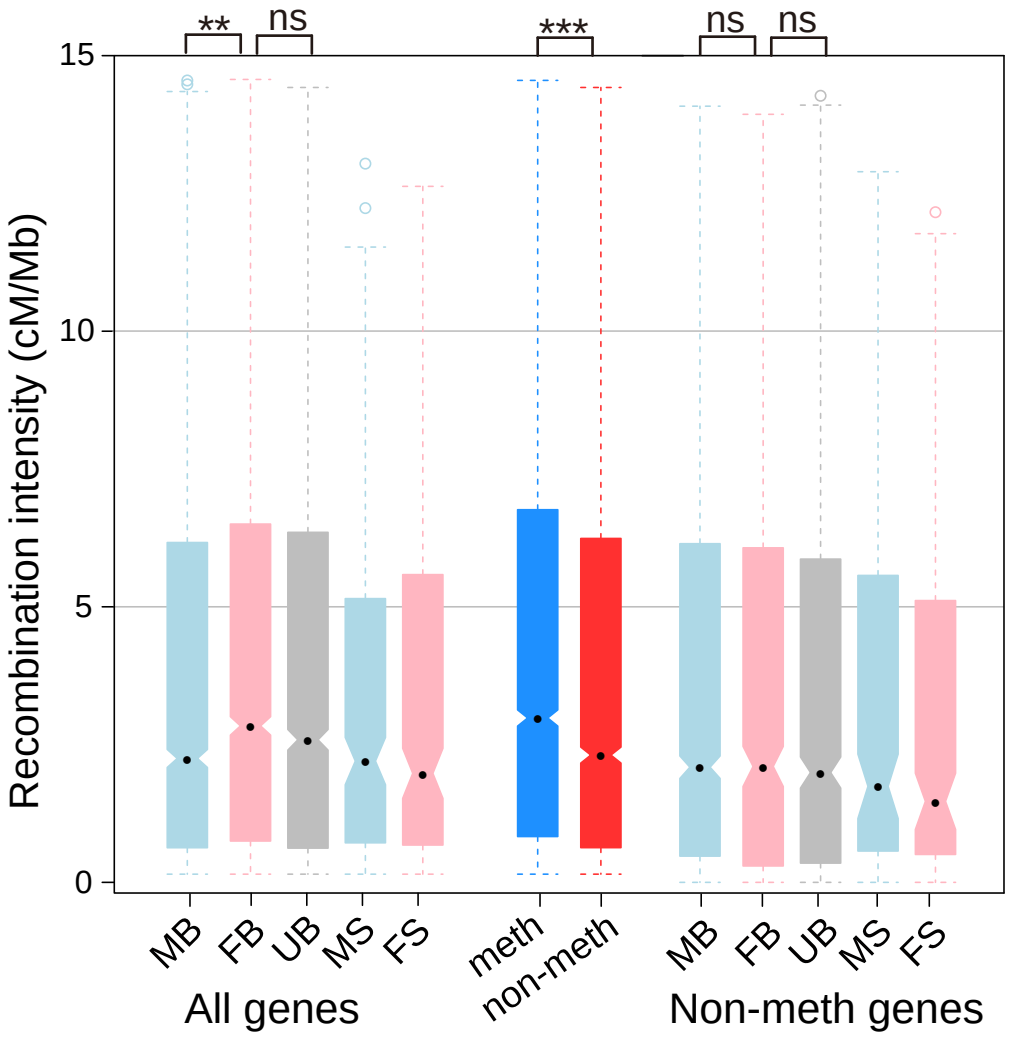

Supporting Table S1. Summary of Illumina RNA-seq data and alignment statistics in *N.vitripennis* and *N.giraulti* female and male adult whole body samples.

Sample ID	Biological replicate #	Tissue	# of reads	adapter %	uniquely mapped reads	unique mapping %
Ngir_f_adult_rep1	1	whole body	56303930	2.07%	49319046	89.45%
Ngir_f_adult_rep2	2	whole body	43947567	1.09%	39432869	90.72%
Ngir_f_adult_rep3	3	whole body	48016561	1.64%	42038120	89.01%
Ngir_m_adult_rep1	1	whole body	61045649	2.72%	51366379	86.49%
Ngir_m_adult_rep2	2	whole body	47950929	1.18%	41748981	88.11%
Ngir_m_adult_rep3	3	whole body	38596761	1.60%	33261106	87.58%
Nvit_f_adult_rep1	1	whole body	65334896	1.89%	59258499	92.45%
Nvit_f_adult_rep2	2	whole body	32732556	1.02%	30310181	93.55%
Nvit_f_adult_rep3	3	whole body	38087649	1.71%	34815152	93.00%
Nvit_m_adult_rep1	1	whole body	75423045	2.24%	67112489	91.02%
Nvit_m_adult_rep2	2	whole body	36552098	1.40%	32361595	89.79%
Nvit_m_adult_rep3	3	whole body	36441305	2.92%	31870320	90.09%

Supporting Table S2. List of selected sex-biased genes for qRT-PCR validation.

Gene ID	Gene annotation	Expression type
Nasvi2EG003640	transport protein Sec16A protein	Control
Nasvi2EG017727	stearoyl-CoA desaturase 5-like	extremely male-biased in both species
Nasvi2EG002222	Acyl-CoA desaturase	male-biased in *N.gir* only
Nasvi2EG005123	Solute carrier family 25 member 35	male-specific in both species
Nasvi2EG009838	Lactase-phlorizin hydrolase	male-specific in both species
Nasvi2EG009041	Hemolymph lipopolysaccharide-binding protein	male-specific in both species
Nasvi2EG012510	chitinase 5 precursor	strongly male-biased in *N.vit* only
Nasvi2EG000206	Unknown singaling protein	extremely male-biased in both species; 10 fold stronger in *N.gir*
Nasvi2EG016119	Cyclin-dependent kinase 9	female-specific in both species
Nasvi2EG014251	DNA mismatch repair protein Msh2 like	extremely female-biased in both species

Supporting Table S3. Members in *Nasonia* fatty acid desaturase gene family and their sex-biased expression status.

GenBank acc. no.	OGS2_IDs	Sex-biased expression	DNA methylation
XP_001602565.1	Nasvi2EG009166	Unbiased	Non-methylated
XP_003425691.1	Nasvi2EG009170	Male-biased; <4 fold	Non-methylated
XP_001599665.2	Nasvi2EG010685	Unbiased	Non-methylated
XP_001607533.2	Nasvi2EG000641	Female-specific; >100 fold	Non-methylated
XP_001599873.1	Nasvi2EG021420	Unbiased	Non-methylated
XP_001602540.1	Nasvi2EG009164	Unbiased	Non-methylated
XP_001599836.1	Nasvi2EG017727	Male-biased; >500 fold	Non-methylated
XP_001599877.2	Nasvi2EG009036	Female-biased; 10 fold	NA
XP_001600683.2	Nasvi2EG011500	Male-biased; <4 fold	Non-methylated
XP_001599899.2	Nasvi2EG009037	Male-biased; 5-8 fold in *N.vit* only	NA
XP_001607893.1	Nasvi2EG002222	Male-biased in *N.gir* head only; 40-fold	Non-methylated
XP_001602289.1	Nasvi2EG009762	Embryo-specific	
XP_001599357.1	Nasvi2EG020749	Unbiased	Non-methylated

Supporting Table S4. Summary of Illumina WGBS-seq data and alignment statistics in *N.vitripennis* and *N.giraulti* female and male adult whole body samples.

Species	Sex	Illumina platform	read length	# of reads	adapter%	bwa parameter	uniquely mapped reads	mapping%
N.vit	Female	HiSeq+GAIIx	84+101	117,506,158	14.41%	n4 o1 e3	51,318,492	51.03%
N.vit	Male	HiSeq+GAIIx	84+101	113,851,688	13.90%	n4 o1 e3	52,726,063	53.79%
N.gir	Female	HiSeq	101	104,409,561	3.35%	n6 o2 e4	47,008,301	46.58%
N.gir	Male	HiSeq	101	123,025,352	4.45%	n6 o2 e4	67,067,188	57.05%

Supporting Table S5. Summary of CpG coverage for different read depth cutoffs in WGBS-seq data.

	N.vit female		*N.vit* male		*N.gir* female		*N.gir* male	
	Count	Percentage	Count	Percentage	Count	Percentage	Count	Percentage
Total CpG*	13451035	-	13451035	-	9742004	-	9742004	-
coverage >= 1	12669187	94.19%	12702115	94.43%	9311952	95.59%	9376945	96.25%
coverage >= 2	12253698	91.10%	12360438	91.89%	9159646	94.02%	9288602	95.35%
coverage >= 10	6791195	50.49%	7236001	53.80%	7569130	77.70%	8425668	86.49%
coverage >= 20	3090093	22.97%	3270086	24.31%	5067529	52.02%	6951256	71.35%
coverage >= 50	447890	3.33%	426043	3.17%	416295	4.27%	1728287	17.74%
average coverage	14.92		15.37		22.84		32.9	

*: CpGs in non-repetitive regions.

Supporting Table S6. Summary of covered and methylated CpGs in *Nasonia* genomes.

	CpG site coverage	# of covered CpG sites	Methylated CpG sites		CpG site coverage	# of covered CpG sites	Methylated CpG sites
N.vit Female	>=1	-	-	*N.gir* Female	>=1	-	-
	>=10	6,791,195	95929 (1.41%)		>=10	7,569,130	92917 (1.23%)
	>=20	3,090,093	68339 (2.21%)		>=20	5,067,529	85082 (1.68%)
	>=50	447,890	15485 (3.46%)		>=50	416,295	22060 (5.30%)
N.vit Male	>=1	-	-	*N.gir* Male	>=1	-	-
	>=10	6,849,195	96437 (1.39%)		>=10	8,425,668	89464 (1.06%)
	>=20	3,270,086	69089 (2.11%)		>=20	6,951,256	80195 (1.15%)
	>=50	426,043	14478 (3.40%)		>=50	1,728,287	28496 (1.65%)

Supporting Table S7. Summary of PyroMark and bisulfite sequencing validation for species-DM gene and sex-DM genes.

Gene ID	Candidate type	Higher methylation in	# DMCpGs	Validation method	Validation results	Spp. Fig.
Nasvi2EG009251	sex-DM gene in *N.vit*	Male	10	Bisulfilte sequencing	Validated	Fig. S8
Nasvi2EG007706	sex-DM gene in *N.vit*	Female	5	PyroMark	Not validated	Fig. S9
Nasvi2EG002107	sex-DM gene in *N.vit*	Female	5	Bisulfilte sequencing	Not validated	Fig. S10
Nasvi2EG008059	sex-DM gene in *N.vit*	Female	5	Bisulfilte sequencing	Not validated	Fig. S11
Nasvi2EG013110	species-DM genes	*N.gir*	46	PyroMark	Validated	Fig. S13
Nasvi2EG030779	species-DM genes	*N.vit*	48	PyroMark	Validated	Fig. S14
Nasvi2EG013343	species-DM genes	*N.vit*	29	PyroMark	Validated	Fig. S15
Nasvi2EG017109	species-DM genes	*N.vit*	17	PyroMark	Validated	Fig. S16
Nasvi2EG028410	species-DM genes	*N.vit*	25	PyroMark	Validated	Fig. S17
Nasvi2EG008123	species-DM genes	*N.gir*	19	PyroMark	Validated	Fig. S18